

19th WEGEMT School

Numerical Simulation of Hydrodynamics:
Ships and Offshore Structures

Offshore Structures

Seakeeping codes AQUADYN and AQUAPLUS

Doctor DELHOMMEAU Gérard
Ecole Centrale de Nantes



E C O L E
Centrale
Nantes

NANTES 20-24 September 1993

THE SEAKEEPING CODES AQUADYN AND AQUAPLUS

G. DELHOMMEAU
L.M.F.-D.H.N.
U.R.A. 1217 du C.N.R.S.
Ecole Centrale de Nantes

I - INTRODUCTION :

This lecture describes briefly the theoretical basis of the two computer codes AQUADYN for seakeeping without forward speed and AQUAPLUS for seakeeping with the approximation of encounter frequency. The code CUVE solving the inner problem will also be described.

The seakeeping problem is the problem of bodies, floating or immersed, in a fluid of infinite or constant finite depth, with or without forward speed and submitted to sinusoidal waves. To describe the problem in mathematical terms, we use the theory of perfect fluid, without viscosity. The theory of nearly perfect fluid allows us to take into account the radiation condition at infinity. First, we set the exact non linear problem, with the exact free surfaces conditions, then this problem is linearized and all quantities are developed up to the second order. We have to solve the hydrodynamic problem at the first order and to apply the results in the mechanical equations at the same order. We will first solve the problem of bodies in waves without forward speed, then the problem of oscillations of fluid in tanks, which is a problem of the same kind as the previous one, and we will conclude by the problem with forward speed and its approximations.

We will describe the computer codes AQUADYN 2.1, CUVE and AQUAPLUS. Several practical examples will be given, with discussion of the main particularities of these codes: recommended number of panels, location and removal of irregular frequencies, need of experimental damping at the resonance of motions, comparison of calculations methods for drift and second order forces.

II - THEORETICAL BASIS :

2.1 General equations for a perfect fluid :

2.1.1 Hypothesis :

The fundamental hypothesis allowing us to describe mathematically the behaviour of a fluid is the continuity hypothesis. Other hypotheses are :

-H1: Strains are proportional to deformation velocities (Newtonian fluid).

-H2: The fluid is homogenous and isotropic. Lamé's viscosity coefficients are slowly varying functions of density and temperature.

-H3: The viscosity coefficients are zero. The density is constant.

-H4: The only external forces are gravity forces. The fluid is initially at rest.

-H5: When there is a free surface, we neglect the surface tension effect and suppose that pressure is constant above free surface.

Hypothesis H1 and H2 lead to the Navier-Stokes equations. With H3, we obtain the perfect fluid equations for an irrotational flow.

2.1.2 General equations :

In the Euler's representation mode, the mass conservation principle gives:

$$\operatorname{div}(\rho \vec{V}) + \frac{\partial \rho}{\partial t} = 0$$

In perfect fluid, we have :

$$\text{div } \vec{V} = 0$$

With H4 hypothesis, we have a potential Φ such as :

$$\vec{V} = \text{grad } \Phi$$

Continuity equation is then :

$$\Delta \Phi = 0$$

The fundamental principle of dynamics is expressed by the Navier-Stokes equations :

$$\frac{1}{\rho} \text{grad } p = \vec{F} - \gamma + \frac{\lambda_1 + \lambda_2}{\rho} \text{grad } (\text{div } \vec{V}) + \frac{\lambda_2}{\rho} \Delta \vec{V}$$

where, in the Euler's representation mode, the acceleration is given by Helmholtz's formula:

$$\gamma = \text{grad } \left(\frac{V^2}{2} \right) + (\text{Rot } \vec{V}) \wedge \vec{V} + \frac{\partial \vec{V}}{\partial t}$$

With H3, we have Euler's equation :

$$\frac{1}{\rho} \text{grad } p = \vec{F} - \gamma$$

H4 gives :

$$\vec{F} = \text{grad } U$$

with $U = -gz$, the z axis being directed upward.

Integration of this equation gives Lagrange's equation, giving pressures at any point of the fluid.

$$\frac{p}{\rho} + gz + \frac{V^2}{2} + \frac{\partial \Phi}{\partial t} = F(t)$$

2.1.3 Boundary conditions :

- Body condition :

On a fluid proof body C , the normal relative velocity is zero. The normal velocity of the fluid is then equal to the normal velocity of a point taken on the body:

$$\vec{V} \cdot \vec{n} |_C = \vec{V}_E \cdot \vec{n} |_C$$

and with the potential :

$$\frac{\partial \Phi}{\partial n} |_C = \vec{V}_E \cdot \vec{n} |_C$$

- Free surface conditions :

Equation of free surface is : $z = \zeta(x, y, t)$

The dynamic condition of free surface is given from Lagrange's equation :

$$gz = F(t) - \frac{p_a}{\rho} - \left(\frac{V^2}{2} + \frac{\partial \Phi}{\partial t} \right) |_{z=\zeta(x,y,t)}$$

For all following problems, we take $p_a = 0$.

The kinematic condition is obtained from continuity hypothesis :

$$\frac{dp}{dt} = 0 = \frac{\partial p}{\partial t} + \vec{V} \cdot \text{grad } p$$

Which gives, combined with Lagrange's formula :

$$\frac{\partial^2 \Phi}{\partial t^2} + g \frac{\partial \Phi}{\partial z} + \frac{\partial V^2}{\partial t} + \frac{1}{2} \vec{V} \cdot \text{grad } V^2 |_{z=\zeta(x,y,t)} = F'(t)$$

- Radiation condition at infinity :

To provide for the unicity of the mathematical solution, it is often necessary to have a supplementary condition expressing the behaviour of the fluid at infinity. One method to obtain this condition is due to Rayleigh and was used by H. Lamb. This is the nearly perfect fluid hypothesis, where we add to the second member of Euler's equation a dissipative term, expressing that the behaviour of the fluid at infinity follows the physical reality, which will be cancelled at the end of the calculations. The latter are transformed as indicated below :

Euler's equation :

$$\frac{1}{\rho} \text{grad } p = \lim_{\epsilon \rightarrow 0^+} (\vec{F} - \gamma - 2 \epsilon' \vec{V})$$

Lagrange's equation :

$$\lim_{\epsilon \rightarrow 0^+} \left(\frac{p}{\rho} + gz + \frac{V^2}{2} + \frac{\partial \Phi}{\partial t} + 2 \epsilon' \Phi \right) = F(t)$$

kinematic and dynamic free surface conditions :

$$\lim_{\epsilon \rightarrow 0^+} \left(\frac{\partial^2 \Phi}{\partial t^2} + g \frac{\partial \Phi}{\partial z} + \frac{\partial V^2}{\partial t} + \frac{1}{2} \vec{V} \cdot \text{grad } \frac{V^2}{2} + 2 \epsilon' \frac{\partial \Phi}{\partial t} + \epsilon' V^2 \right) |_{z=\zeta(x,y,t)} = F'(t)$$

$$\zeta = \lim_{\epsilon \rightarrow 0^+} \frac{1}{g} \left[- \frac{\partial \Phi}{\partial t} - \frac{V^2}{2} - 2 \epsilon' \Phi + F'(t) \right]$$

- Absolute values expressed in moving axis :

Previous boundary conditions can be written in a moving frame parallel to the absolute frame and moving with the velocity V_0 . In this case, we have :

$$\frac{\partial}{\partial t} |_{\text{fixed axis}} = \frac{\partial}{\partial t} |_{\text{moving axis}} - \vec{V}_0 \cdot \text{grad} |_{\text{moving axis}}$$

Other derivatives in respect with space variables are the same in the two axes.

2.1.4 Similitude laws :

The similitude of perfect fluid submitted to gravity forces with a free surface makes it necessary to respect the Reech-Froude number :

$$Fn = \frac{V}{\sqrt{gL}}$$

If we consider two fluids of density ρ_1 and ρ_2 , with lengths L_1 and L_2 , with gravity fields g_1 and g_2 , similitude of velocities give :

$$\text{speed : } \frac{V_1}{\sqrt{g_1 L_1}} = \frac{V_2}{\sqrt{g_2 L_2}}$$

and for mass and time :

$$\text{mass : } \frac{M_1}{\rho_1 L_1^3} = \frac{M_2}{\rho_2 L_2^3}$$

$$\text{time : } \frac{1}{T_1} \sqrt{\frac{L_1}{g_1}} = \frac{1}{T_2} \sqrt{\frac{L_2}{g_2}}$$

and for other quantities :

displacement : $\frac{X_1}{L_1} = \frac{X_2}{L_2}$

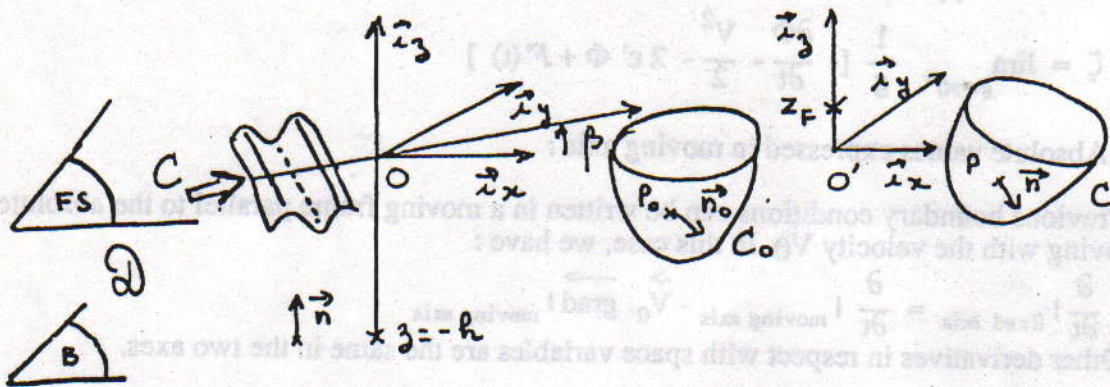
acceleration : $\frac{\gamma_1}{g_1} = \frac{\gamma_2}{g_2}$

force : $\frac{F_1}{\rho_1 g_1 L_1^3} = \frac{F_2}{\rho_2 g_2 L_2^3}$

All calculations made for a given fluid will be available for a fluid in similitude. If density and gravity are the same, these laws give the variation of quantities with geometric scale.

2.2 Equations of mechanics applied to the problem without forward speed :

2.2.1 System of coordinates :



- O : Origin of the fixed axis.
- O' : Origin of axis moving with the body and parallel to the fixed axis.
The height of free surface at rest in these axis is z_F .
- ϵ' : Vanishing viscosity of nearly perfect fluid.
- ϵ : Little parameter of the development in series.

2.2.2 Equations of the problem :

The equations of the whole problem in perfect fluid are :

$$\left\{ \begin{array}{l} \Delta\Phi = 0 \\ \frac{\partial\Phi}{\partial n} \Big|_C = \vec{V}_E \cdot \vec{n} \Big|_C \\ \frac{\partial\Phi}{\partial z} \Big|_{z=-h} = 0 \\ \Phi \rightarrow \Phi_I \text{ at infinity} \\ \lim_{\epsilon' \rightarrow 0^+} \left[\frac{\partial^2\Phi}{\partial t^2} + g \frac{\partial\Phi}{\partial z} + \frac{\partial V^2}{\partial t} + \frac{1}{2} \vec{V} \cdot \text{grad} V^2 + 2\epsilon' \frac{\partial\Phi}{\partial t} + \epsilon' V^2 \right]_{z=\zeta(x,y,t)} = F(t) \\ \zeta = \lim_{\epsilon' \rightarrow 0^+} \left[-\frac{1}{g} \frac{\partial\Phi}{\partial t} + \frac{V^2}{2} + 2\epsilon' \Phi - F(t) \right]_{z=\zeta(x,y,t)} \end{array} \right.$$

If we develop the problem in perturbation series of the little parameter ϵ , we have :

$$\Phi = \epsilon \Phi^{(1)} + \epsilon^2 \Phi^{(2)} + o(\epsilon^2) = \Phi_1 + \Phi_2 + o(\epsilon^2)$$

$$\vec{V} = \text{grad} \Phi = \epsilon \vec{V}^{(1)} + \epsilon^2 \vec{V}^{(2)} + o(\epsilon^2) = \vec{V}_1 + \vec{V}_2 + o(\epsilon^2)$$

where $o(\epsilon^2)$ are terms of order greater than ϵ^2

2.2.3 Hydrodynamic problems at first and second order :

Developing the incident wave, the body condition and the free surface condition at second order, we have the following equations :

For the incident wave :

$$F_{I1} = -\frac{ag}{\omega} \frac{\text{ch } m_0(z+h)}{\text{ch } m_0 h} \cos [m_0(x \cos \beta + y \sin \beta) - \omega t]$$

with : $\omega^2 = gm_0 \text{th } m_0 h$, and

$$F_{I2} = -\frac{3m_0 a^2 g}{8\omega} \frac{\text{ch } 2m_0(z+h)}{\text{sh}^3 m_0 h \text{ch } m_0 h} \sin 2[m_0(x \cos \beta + y \sin \beta) - \omega t]$$

$$F(t) = F_2 = \frac{m_0 a^2 g}{4} \frac{1}{\text{sh } m_0 h \cdot \text{ch } m_0 h}$$

For the hydrodynamic problem at first and second order :

$$\left\{ \begin{array}{l} \Delta \Phi_1 = 0 \\ \frac{\partial \Phi_1}{\partial n_0} \Big|_{C_0} = \vec{V}_{E1} \cdot \vec{n}_0 \Big|_{C_0} \\ \frac{\partial \Phi_1}{\partial z} \Big|_{z=-h} = 0 \\ \Phi_1 \rightarrow \Phi_{I1} \text{ at infinity} \\ \lim_{\epsilon' \rightarrow 0^+} \frac{\partial^2 \Phi_1}{\partial t^2} + 2\epsilon' \frac{\partial \Phi_1}{\partial t} + g \frac{\partial \Phi_1}{\partial z} \Big|_{z=0} = E\Phi_1 \Big|_{z=0} = 0 \\ \zeta_1 = -\frac{1}{g} \frac{\partial \Phi_1}{\partial t} \Big|_{z=0} \end{array} \right.$$

$$\left\{ \begin{array}{l} \Delta \Phi_2 = 0 \\ \frac{\partial \Phi_2}{\partial n_0} \Big|_{C_0} = \vec{V}_{E2} \cdot \vec{n}_0 \Big|_{C_0} + \vec{V}_{E1} \cdot \vec{n}_1 \Big|_{C_0} - \frac{\partial \Phi_1}{\partial n_1} \Big|_{C_0} - P_0 \vec{P}_1 \cdot \text{grad} \vec{V}_{E1} \cdot \vec{n}_0 \Big|_{C_0} \\ \frac{\partial \Phi_2}{\partial z} \Big|_{z=-h} = 0 \\ \Phi_2 \rightarrow \Phi_{I2} \text{ at infinity} \\ E\Phi_2 \Big|_{z=0} = -2g \text{grad} \Phi_1 \cdot \text{grad} \frac{\partial \Phi_1}{\partial t} \Big|_{z=0} + \frac{\partial \Phi_1}{\partial t} \frac{\partial (E\Phi_1)}{\partial z} \Big|_{z=0} + \lim_{\epsilon' \rightarrow 0^+} \epsilon' (\text{grad} \Phi_1)^2 \Big|_{z=0} \\ \zeta_2 = -\frac{1}{g} \left[\frac{\partial \Phi_2}{\partial t} + \zeta_1 \frac{\partial}{\partial z} \frac{\partial \Phi_1}{\partial t} + \frac{\vec{V}_1^2}{2} - F_2 \right] \Big|_{z=0} \end{array} \right.$$

The total potential at second order being :

$$\Phi = \Phi_1 + \Phi_2 + o(\epsilon^2)$$

2.2.4 Description of the motion of a body :

To describe the motion of a body, we divide the motion into two parts, translations and rotations.

Vector translation : $\vec{\tau} = O\vec{O}'$

Vector rotation : $\vec{\theta} = \theta\vec{q}$ around \vec{q}

We can represent the rotation of any vector by:

$$R(\vec{u}) = \vec{u} + \frac{\sin \theta}{\theta} \vec{\theta} \wedge \vec{u} + \frac{1 - \cos \theta}{\theta^2} \vec{\theta} \wedge (\vec{\theta} \wedge \vec{u})$$

The displacements of any point of the body in respect to its location at rest are :

$$P_0\vec{P}_1^{(0)} = \vec{0}$$

$$P_0\vec{P}_1 = \vec{\tau}_1 + R_1(O\vec{P}_0) = \vec{\tau}_1 + \vec{\theta}_1 \wedge O\vec{P}_0$$

$$P_0\vec{P}_2 = \vec{\tau}_2 + R_2(O\vec{P}_0) = \vec{\tau}_2 + \vec{\theta}_2 \wedge O\vec{P}_0 + \frac{1}{2} \vec{\theta}_1 \wedge (\vec{\theta}_1 \wedge O\vec{P}_0)$$

2.2.5 Pressures, forces:

Pressures at different orders are obtained from Lagrange's equation :

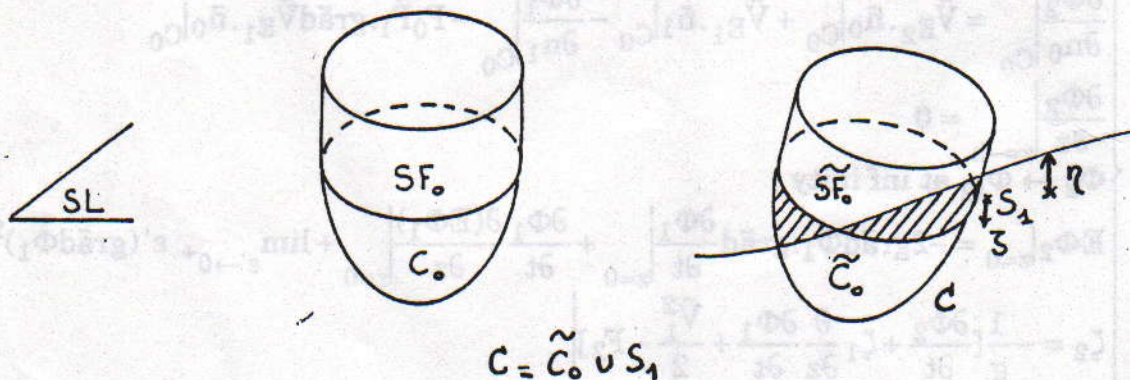
$$P_0 = -\rho g(z - z_F)$$

$$P_1 = -\rho g P_0 \vec{P}_1 \cdot \vec{i}_z - \rho \frac{\partial \Phi_1}{\partial t}$$

$$P_2 = -\rho g P_0 \vec{P}_2 \cdot \vec{i}_z - \rho \frac{\partial \Phi_2}{\partial t} - \rho P_0 \vec{P}_1 \cdot \text{grad} \frac{\partial \Phi_1}{\partial t} - \frac{1}{2} \rho (\text{grad} \Phi_1)^2 + F_2$$

$$F_2 = \frac{m_0 a^2 g}{4} \frac{1}{\text{sh } m_0 h \cdot \text{ch } m_0 h}$$

The position taken by the body during its motion are given on the figure below :



With the following hypothesis on the order of magnitude of the integrals, the forces exerted by the fluid on the body can be written :

$$\iint_{S_1} = O(\epsilon), \quad \iint_{C_0} = O(1)$$

$$\bar{n}_g = \bar{n}_0 \text{ for the forces}$$

$$\bar{n}_g = O\bar{P}_0 \wedge \bar{n}_0 \text{ for the moments around } O' \text{ moving with the body}$$

$$\bar{F}_{g0} = - \iint_{C_0} p_0 \bar{n}_g dS$$

$$\bar{F}_{g1} = \bar{\theta}_1 \wedge \bar{F}_{g0} - \iint_{C_0} p_1 \bar{n}_g dS - \iint_{S_1} p_0 \bar{n}_g dS$$

$$\bar{F}_{g2} = \bar{\theta}_2 \wedge \bar{F}_{g0} + \frac{1}{2} \bar{\theta}_1 \wedge (\bar{\theta}_1 \wedge \bar{F}_{g0}) + \bar{\theta}_1 \wedge (\bar{F}_{g1} - \bar{\theta}_1 \wedge \bar{F}_{g0}) - \iint_{C_0} p_2 \bar{n}_g dS - \iint_{S_1} p_1 \bar{n}_g dS$$

2.2.6 External forces :

External forces can be divided into hydrostatic forces and hydrodynamic forces. The hydrostatic forces are the resultant of gravity forces and buoyancy forces. For a floating body at equilibrium we have :

$$Mg = \rho g V_0, \quad X_{C_0} = X_{G_0}, \quad Y_{C_0} = Y_{G_0}$$

G_0 being the gravity centre and C_0 the hull centre, defined by :

$$O\bar{P}_0 = X\bar{i}_x + Y\bar{i}_y + Z\bar{i}_z, \quad O\bar{C}_0 = \frac{1}{V_0} \int_{V_0} O\bar{P}_0 dV, \quad O\bar{G}_0 = \frac{1}{M} \int_{V_0} O\bar{P}_0 dm$$

The hydrostatic restoring matrix is defined by :

$$\bar{S} = \begin{bmatrix} 0 & 0 & 0 & 0 & 0 & 0 \\ 0 & 0 & 0 & 0 & 0 & 0 \\ 0 & 0 & S_{33} & S_{34} & S_{35} & 0 \\ 0 & 0 & S_{43} & S_{44} & S_{45} & 0 \\ 0 & 0 & S_{53} & S_{54} & S_{55} & 0 \\ 0 & 0 & 0 & 0 & 0 & 0 \end{bmatrix}$$

with :

$$S_{33} = \rho g \iint_{SF_0} dS = \rho g S F_0$$

$$S_{34} = \rho g \iint_{SF_0} Y dS = S_{43}$$

$$S_{35} = -\rho g \iint_{SF_0} X dS = S_{53}$$

$$S_{44} = \rho g \iint_{SF_0} Y^2 dS + \rho g V_0 (Z_{C_0} - Z_{G_0})$$

$$S_{45} = -\rho g \iint_{SF_0} XY dS = S_{54}$$

$$S_{55} = \rho g \iint_{SF_0} X^2 dS + \rho g V_0 (Z_{C_0} - Z_{G_0})$$

The hydrostatic forces at a point O' moving with the body, are given by :

$$\vec{F}_{hs0} = \vec{0}$$

$$\vec{F}_{hs1} = -[S_{33}\tau_{z1} + S_{34}\theta_{x1} + S_{35}\theta_{y1}] \cdot \vec{i}_z$$

$$\vec{F}_{hs2} = \vec{\theta}_1 \wedge \vec{F}_{hs1} - [S_{33}(\tau_{z2} - \frac{\theta_{x1}^2 + \theta_{y1}^2}{2} z_F) + S_{34}(\tau_{x2} + \frac{\theta_{y1} \cdot \theta_{z1}}{2}) + S_{35}(\tau_{y2} - \frac{\theta_{x1} \cdot \theta_{z1}}{2})] \cdot \vec{i}_z$$

$$\vec{M}_{hs0}(O') = \vec{0}$$

$$\vec{M}_{hs1}(O') = -[S_{43}\tau_{z1} + S_{44}\theta_{x1} + S_{45}\theta_{y1}] \cdot \vec{i}_x$$

$$-[S_{53}\tau_{z1} + S_{54}\theta_{x1} + S_{55}\theta_{y1}] \cdot \vec{i}_y$$

$$\vec{M}_{hs2}(O') = -[S_{43}(\tau_{z2} - \frac{\theta_{x1}^2 + \theta_{y1}^2}{2} z_F) + S_{44}(\tau_{x2} + \frac{\theta_{y1} \cdot \theta_{z1}}{2}) + S_{45}(\tau_{y2} - \frac{\theta_{x1} \cdot \theta_{z1}}{2})] \cdot \vec{i}_x$$

$$-[S_{53}(\tau_{z2} - \frac{\theta_{x1}^2 + \theta_{y1}^2}{2} z_F) + S_{54}(\tau_{x2} + \frac{\theta_{y1} \cdot \theta_{z1}}{2}) + S_{55}(\tau_{y2} - \frac{\theta_{x1} \cdot \theta_{z1}}{2})] \cdot \vec{i}_y + \vec{\theta}_1 \wedge \vec{M}_{hs1}(O')$$

The transportation at a point O fixed being done by :

$$\vec{M}_{hs2}(O) = \vec{M}_{hs2}(O') + \vec{\tau}_1 \wedge \vec{F}_{hs1}$$

And the hydrodynamic forces at a point O' moving with the body, by :

$$\zeta_1 = -\frac{1}{g} \frac{\partial \Phi_1}{\partial t} \Big|_{z=0} : \text{wave height ; } Z_1 = P_0 \vec{P}_1 \cdot \vec{i}_z \Big|_{z=0} : \text{vertical displacement at free surface}$$

$$\vec{n}_g = \vec{n}_0 \text{ for the forces}$$

$$\vec{n}_g = O\vec{P}_0 \wedge \vec{n}_0 \text{ for the moments around } O' \text{ moving with the body}$$

$$\vec{F}_{hd0} = \vec{0}$$

$$\vec{F}_{hd1} = - \iint_{C_0} p_1 \vec{n}_g \, dS = \rho \iint_{C_0} \frac{\partial \Phi_1}{\partial t} \vec{n}_g \, dS$$

$$\vec{F}_{hd2} = \vec{\theta}_1 \wedge \vec{F}_{hd1} + \rho \iint_{C_0} \left[\frac{\partial \Phi_2}{\partial t} + P_0 \vec{P}_1 \cdot \text{grad} \frac{\partial \Phi_1}{\partial t} + \frac{1}{2} \rho (\text{grad} \Phi_1)^2 - F_2 \right] \vec{n}_g \, dS - \frac{\rho g}{2} \int_{\Gamma_0} (\zeta_1 - Z_1)^2 \vec{n}_g \, dS$$

The transportation at a point O fixed being done by :

$$\vec{M}_{hd2}(O) = \vec{M}_{hd2}(O') + \vec{\tau}_1 \wedge \vec{F}_{hd1}$$

2.2.7 Inertial forces :

The inertial forces, developed at first order give :

$$\vec{F}_{M_1} = M\vec{\ddot{r}}_1 + M\vec{\theta}_1 \wedge O\vec{G}_0$$

$$\vec{M}_{M_1} = MO\vec{G}_0 \wedge \vec{\ddot{r}}_1 + \int_M [\vec{\theta}_1(O\vec{P}_0)^2 - O\vec{P}_0(O\vec{P}_0 \cdot \vec{\theta}_1)] dm$$

$$I_{44} = \int_M (Y^2 + Z^2) dm ; I_{55} = \int_M (Z^2 + X^2) dm ; I_{66} = \int_M (X^2 + Y^2) dm$$

$$I_{45} = I_{54} = - \int_M XY dm ; I_{46} = I_{64} = - \int_M XZ dm ; I_{56} = I_{65} = - \int_M YZ dm$$

$$\vec{P} = \begin{bmatrix} M & 0 & 0 \\ 0 & M & 0 \\ 0 & 0 & M \end{bmatrix} ; \vec{I} = \begin{bmatrix} I_{44} & I_{45} & I_{46} \\ I_{54} & I_{55} & I_{56} \\ I_{64} & I_{65} & I_{66} \end{bmatrix} ; \vec{T} = \begin{bmatrix} 0 & Mz_{G_0} & -My_{G_0} \\ -Mz_{G_0} & 0 & Mx_{G_0} \\ My_{G_0} & -Mx_{G_0} & 0 \end{bmatrix}$$

$$\begin{bmatrix} \vec{F}_{M_1} \\ \vec{M}_{M_1} \end{bmatrix} = \begin{bmatrix} \vec{P} & \vec{T} \\ -\vec{T} & \vec{I} \end{bmatrix} \begin{bmatrix} \vec{\ddot{r}}_1 \\ \vec{\theta}_1 \end{bmatrix} = \vec{M} \begin{bmatrix} \vec{\ddot{r}}_1 \\ \vec{\theta}_1 \end{bmatrix}$$

2.3 Solution of the hydrodynamic problem at first order :

2.3.1 Decomposition of the problem :

For the problem of N bodies oscillating independently in waves, we have at first order :

$$\left\{ \begin{array}{l} \Delta\Phi = 0 \\ \frac{\partial\Phi}{\partial n} \Big|_{\Sigma_i} = \vec{V}_{E_i} \cdot \vec{n} \Big|_{\Sigma_i} ; i = 1, 2, \dots, N \\ \frac{\partial\Phi}{\partial z} \Big|_{z=-h} = 0 \\ \Phi \rightarrow \Phi_I \text{ at infinity} \\ \lim_{\epsilon' \rightarrow 0^+} \frac{\partial^2\Phi}{\partial t^2} + 2\epsilon' \frac{\partial\Phi}{\partial t} + g \frac{\partial\Phi}{\partial z} \Big|_{z=0} = E\Phi \Big|_{z=0} = 0 \\ \zeta = -\frac{1}{g} \frac{\partial\Phi}{\partial t} \Big|_{z=0} \end{array} \right.$$

$$\Phi_I = -\frac{ag \operatorname{ch} m_0(z+h)}{\omega \operatorname{ch} m_0 h} \cos [m_0(x \cos \beta + y \sin \beta) - \omega t]$$

and : $\omega^2 = gm_0 \operatorname{th} m_0 h$

with the unknown velocities obtained from unknown amplitudes of motions :

$$\bar{V}_{Ei} = \bar{V}_{Ei}^* \cos \omega t + \bar{V}_{Ei}^{**} \sin \omega t = \sum_{q=1}^6 \bar{V}_{Ei}^q$$

and :

$$\begin{aligned} \bar{V}_{Ei} = & -\omega \sin \omega t \left[\sum_{q=1}^3 A_i^q \bar{e}_q + \sum_{q=4}^6 A_i^q (\bar{e}_{q-3} \wedge O\bar{P}_0) \right] \\ & + \omega \cos \omega t \left[\sum_{q=1}^3 A_i^q \bar{e}_q + \sum_{q=4}^6 A_i^q (\bar{e}_{q-3} \wedge O\bar{P}_0) \right] \end{aligned}$$

with :

$$A_i^q = A_i^q \cos \omega t + A_i^q \sin \omega t$$

$\bar{e}_q, q=1,2,3$ are the unit vector of the axis x,y and z.

Considering a perturbation potential, this problem can be divided into N+1 problems :

$$\Phi = \Phi^* \cos \omega t + \Phi^{**} \sin \omega t$$

$$\Phi = \Phi_I + \Phi_p$$

$$\Phi_p = \Phi_D + \sum_{i=1}^N \Phi_{Ri}$$

One diffraction problem, for which the body condition is :

$$\left. \frac{\partial \Phi_D}{\partial n} \right|_{\Sigma_i} = - \left. \frac{\partial \Phi_I}{\partial n} \right|_{\Sigma_i} ; i = 1, 2, \dots, N$$

and 2N radiation problems, for which the body condition are :

$$\left. \frac{\partial \Phi_{Ri}}{\partial n} \right|_{\Sigma_i} = (\bar{V}_{Ei}^* \cos \omega t + \bar{V}_{Ei}^{**} \sin \omega t) \Big|_{\Sigma_i} ; i = 1, 2, \dots, N$$

$$\left. \frac{\partial \Phi_{Ri}}{\partial n} \right|_{\Sigma_j} = 0 ; j \neq i$$

which are known after having solved only N elementary radiation problems :

$$\left. \frac{\partial \Phi^q_{Ri}}{\partial n} \right|_{\Sigma_i} = \bar{V}^q_{Ei} \cos \omega t \Big|_{\Sigma_i} ; |\bar{V}^q_{Ei}| = 1$$

$$\left. \frac{\partial \Phi^q_{Ri}}{\partial n} \right|_{\Sigma_j} = 0 ; j \neq i$$

2.3.2 Complex notation :

For quantities varying sinusoidally with time, we can use the complex notation :

$$A = A^* \cos \omega t + A^{**} \sin \omega t = \text{Re } \bar{A} e^{-i\omega t} ; \bar{A} = A^* + iA^{**}$$

$$\langle A.B \rangle = \frac{1}{2} \text{Re}(\bar{A} \bar{B}) = \frac{1}{2} \text{Re}(\bar{B} \bar{A}) = \frac{1}{4} \text{Re}(\bar{A} \bar{B} + \bar{B} \bar{A})$$

where $\langle A.B \rangle$ is the average value in time of the product A.B.

2.3.3 Solution of the problem by boundary element method :

To solve these problems, we use the boundary element method, with Green's function allowing to take into account the boundary conditions on body, bottom and free surface.

There are two main differences between all the diffraction-radiation programs :

a) The first difference is in the type of singularity distribution used. In the program AQUADYN, we use a mixed distribution of sources and normal dipoles, where the sources are known from the body condition and the normal dipoles are unknown. The solution of the problem is the potential. The velocities outside of the bodies, which are not known by the body condition need computation of influence coefficients of velocity for normal dipoles, a process known as being of poor accuracy (derivative operator) . In the AQUAPLUS program, we use only a distribution of sources. The solution of the problem is the velocity and the potential is calculated from the sources by influence coefficients with a good accuracy (integration operator) .

b) The second difference is in the way to compute Green's function. and the discretized influence coefficients integrated on a panel. In the general case, we can write:

$$C = C_1 + C_2$$

$$C_1 = \iint_S f\left(\frac{1}{MM'_1}\right) dS(M'_1); M'_1(x', y', z'_1)$$

$$C_2 = \iint_S \left[\int_{-\frac{\pi}{2}}^{\frac{\pi}{2}} \ddot{g}(\xi) d\theta \right] dS(M')$$

$$\xi = A[z + \epsilon z' + i\omega] \quad ; \quad \omega = (x - x') \cos \theta + (y - y') \sin \theta$$

Due to the cylindrical symmetry of the Green's function, we can also write :

$$\int_{-\frac{\pi}{2}}^{\frac{\pi}{2}} \ddot{g}(\xi) d\theta = \int_{-\frac{\pi}{2}}^{\frac{\pi}{2}} \ddot{g}(\zeta) d\theta$$

with: :

$$\zeta = Z + iR \cos \theta \quad ; \quad Z = A(z + \epsilon z') \quad ; \quad R = A\sqrt{(x - x')^2 + (y - y')^2}$$

The terms C_1 are calculated analytically by classical Hess and Smith formulas (1966) or similar approximations (P. Guével: 1975) [14].

For the terms C_2 , there is a choice:

- We can first compute numerically the simple integral, and then analytically the double integral on S. This choice was made for the first version of AQUADYN (1976) [19].

- We can first compute the simple integral in θ and then compute numerically the double integral on S. In practice, due to the slow variation of the integration term on the panel, the double integral on S can be approximated by only one point formula, which makes this method very efficient. There is also two ways of computing the simple integral in θ :

a)- we can approximate the integral by several analytical formulas, each available in a domain of variation of R and Z, as proposed by F. Noblesse (1982) and J.N. Newman (1985)[17].

b)- we can obtain the same results by using a interpolation into a file of four elementary functions of the two variables R and Z , created only one time and loaded at each execution of the program [21]. This file is available both for infinite and finite water depth. The size of the file is less than 512 KBytes and this method is used in the codes AQUADYN 2.1 and AQUAPLUS. (1987) with a quadratic interpolation. The resulting computation time are of the same order as with analytical formulas, but the development effort is less for the second method.

The asymptotic values of the Green functions are obtained by the anti mirror image ($1/R - 1/R_1$ for $T=0$) and the mirror image ($1/R + 1/R_1$: double model for $T=\infty$).

2.3.4 Discretization of integral equations :

When written on the control point of each panel of a body, the integral equations of the boundary element method are transformed in linear systems, we have :

For the mixed distribution , N being the total number of panels on the bodies:

$$\frac{\tilde{\mu}_i}{2} + \sum_{j=1}^N \tilde{\mu}_j \tilde{D}_{ij} = \sum_{j=1}^N \frac{\partial \tilde{\Phi}_e}{\partial n} \Big|_{M_j} \tilde{S}_{ij}$$

And for the source distribution :

$$\frac{\tilde{\sigma}_i}{2} + \sum_{j=1}^N \tilde{\sigma}_j \tilde{K}_{ij} = \frac{\partial \tilde{\Phi}_e}{\partial n} \Big|_{M_i}$$

The potential of sources are obtained by :

$$\tilde{\Phi} \Big|_{M_i} = - \sum_{j=1}^N \tilde{\sigma}_j \tilde{S}_{ij}$$

and the influence coefficients are obtained by:

$$\tilde{S}_{ij} = \frac{1}{4\pi} \iint_S \tilde{S}(M_i, M') ds(M')$$

$$\tilde{D}_{ij} = -\frac{1}{4\pi} \iint_S \frac{\partial}{\partial n} \Big|_{M'} \tilde{S}(M_i, M') ds(M') \quad , \quad \tilde{D}_{ii} = 0.5$$

$$\tilde{K}_{ij} = -\frac{1}{4\pi} \frac{\partial}{\partial n} \Big|_{M_i} \iint_S \tilde{S}(M_i, M') ds(M') \quad , \quad \tilde{K}_{ii} = 0.5$$

\tilde{S} being the Green's function of the problem.

For the elementary radiation problem $\tilde{\Phi}_{R_i}^q$:

$$\frac{\partial \tilde{\Phi}_e}{\partial n} \Big|_{\Sigma_i} = \sigma_i^q ; \text{ with } \sigma_i^q = \begin{cases} \tilde{e}_q \cdot \tilde{n} & q = 1, 2, 3 \\ (\tilde{e}_{q-3} \wedge O\tilde{P}_0) \cdot \tilde{n} & q = 4, 5, 6 \end{cases}$$

For the diffraction problem $\tilde{\Phi}_D$:

$$\frac{\partial \tilde{\Phi}_e}{\partial n} \Big|_{\Sigma_i} = - \frac{\partial \tilde{\Phi}_I}{\partial n} \Big|_{\Sigma_i}$$

All coefficients of the linear systems are complex. They can be written in real form by separating the contribution of terms in sinus and terms in cosines, but the real system will have twice as many unknowns as the complex one. The computation times of a real system of order 2M is in $8M^3$ and those of a complex system of order M is $4M^3$. The complex notation is not only a writing facility, it also saves computation time.

2.3.5 Irregular frequencies :

The previous integral equations are Fredholm's integral equations of the second kind. These equations have generally an unique solution, except for certain discrete frequencies when the solution of the inner associate problem is not identical to zero.

$$\begin{cases} \Delta\Phi = 0 \\ E\Phi|_{z=0} = 0 \\ \Phi|_{\Sigma} = 0 \end{cases}$$

This can occur only when the body is not fully immersed. The general principle to suppress these irregular frequencies is to write on the free surface a supplementary condition which makes the potential (or its normal derivative in z) is zero at certain points of the free surface. In practice, these frequencies are generally rather high and are not always in the domain of calculation for wave problems. We can approximate the period of the lowest irregular frequency by the formula

$$T = 2\pi \sqrt{\frac{\text{th}\left(\frac{\pi H}{L} \sqrt{\frac{L^2}{B^2} + 1}\right)}{\frac{\pi g}{L} \sqrt{\frac{L^2}{B^2} + 1}}}$$

Handwritten notes: ≈ 2.6 , ≈ 1.42 , ≈ 5.27

$\omega_n = 1, 2$

where L,B are the length and breadth at waterline and H is the draft.

For L=20 m and B=6 m, we have T=2.6 s and for Land B=90 m and H=40 m, T=8.857 s.

In practice, the influence of irregular frequencies is identified in a narrow strip of approximately 0.2 s in period, depending of the mesh (decreasing with refined mesh). This region is slightly greater for source distribution than for mixed distribution for three dimensional cases.

2.3.6 Radiation problems :

The elementary radiation problem is the problem of a body with a forced sinusoidal motion, in initially calm water. The forces on the body and on the other bodies are obtained from Lagrange's equation:

For the motion q of body i, we have :

$$\tilde{p} = \rho\omega^2 \sum_{q=1}^6 A_i^q \tilde{\Phi}_{Ri}^q$$

Force p on the body j is given by :

$$F_{Rj}^p = - \sum_{q=1}^6 \{M_{ij}^{pq} [-\omega^2 (A_i^{q*} \cos \omega t + A_i^{q**} \sin \omega t)]$$

$$+ B_{ij}^{pq} [-\omega (A_i^{q*} \sin \omega t - A_i^{q**} \cos \omega t)]\}$$

$$M_{ij}^{pq} = -\rho \iint_{\Sigma_j} \Phi_{Ri}^{q*} \frac{\partial \Phi_{Ri}^{p*}}{\partial n} dS$$

$$B_{ij}^{pq} = -\rho\omega \iint_{\Sigma_j} \Phi_{Ri}^{q**} \frac{\partial \Phi_{Ri}^{p*}}{\partial n} dS$$

$$\tilde{M}_{ij}^{pq} = M_{ij}^{pq} + \frac{i}{\omega} B_{ij}^{pq}$$

Properties :

$$M_{ij}^{pq} = M_{ji}^{qp} ; B_{ij}^{pq} = B_{ji}^{qp} ; B_{ii}^{pp} \geq 0 ; M_{ii}^{pp} = ?$$

The diagonal of the matrix of damping coefficient must be positive, and the matrices symmetrical by blocks. This gives a good estimation of the numerical error due to discretization.

In practice, we also find that the diagonal of the added mass matrix is positive, except at certain frequencies for special geometries (catamaran or moon pool)..

The terms of added mass and damping coefficients are the resultant of dynamic pressures and are not invariant. The added mass and damping coefficients are function of the period of the motion and of water depth. At high frequencies ($T \rightarrow \infty$, acoustic in incompressible water) and at low frequencies ($T \rightarrow 0$) the damping coefficients are zero. The asymptotic values of the added mass coefficients are obtained by the anti mirror image ($1/R - 1/R_1$) and the mirror image ($1/R + 1/R_1$: double model) in Green's functions. For a group of N bodies, the added mass and damping coefficient matrices are two real matrices ($6N \times 6N$) or one complex matrix of the same dimension.

2.3.7 Diffraction problem :

Excitation forces come from diffraction potential and incident potential:

$$\tilde{\Phi}_{ex} = \tilde{\Phi}_D + \tilde{\Phi}_I$$

Force q on the body i is given by :

$$F_{exi}^q = i\rho\omega \iint_{\Sigma_i} (\tilde{\Phi}_D + \tilde{\Phi}_I) \frac{\partial \Phi_{Ri}^{q*}}{\partial n} dS$$

Or by Haskind's formula :

$$F_{exi}^q = -i\rho\omega \iint_{\Sigma} (\tilde{\Phi}_I \frac{\partial \tilde{\Phi}_{Ri}^q}{\partial n} - \tilde{\Phi}_{Ri}^q \frac{\partial \tilde{\Phi}_I}{\partial n}) dS$$

$$\Sigma = \Sigma_1 \cup \Sigma_2 \cup \dots \cup \Sigma_N$$

The part of excitation forces due to the incident wave are often called Froude-Krylov forces.

The excitation forces can be calculated by direct pressure integration of the diffraction and incident potentials or after having solved the radiation problem, without having solved a supplementary problem, by the Haskind's formula. When we use this formula, we don't know the local pressures on the bodies, which forbid to reach second order forces. This formula is only used to verify the quality of the numerical solution by pressure integration. Unfortunately, the agreement with pressure integration is too good for this comparison to be useful.

2.3.8 Equations of motions :

The unknowns are the motions of the bodies. If we make the sum of all forces exerted on the bodies, we have :

$$F_M = F_{hs} + F_R + F_{ex} + F_L$$

where F_M are inertial forces, F_{hs} the hydrostatic restoring force, F_R the radiation forces, F_{ex} the excitation forces (the sum of Froude-Krylov forces and diffraction forces) and F_L external linear forces which may be due to the stiffness and the damping of a mooring system.

The line corresponding to the motion q of body i is written :

$$-\omega^2 \sum_{p=1}^6 \bar{M}_{pq} \tilde{A}_i + \sum_{p=1}^6 \bar{S}_{pq} \tilde{A}_i - \omega^2 \sum_{j=1}^N \sum_{p=1}^6 \tilde{M}_{pq} \tilde{A}_j + \sum_{p=1}^6 \tilde{F}_{Lpq} \tilde{A}_i = F_{exi}$$

The linear system for N bodies is :

$$\begin{bmatrix} \bar{S}_1 + \tilde{F}_{L11} - \omega^2 (\bar{M}_1 + \tilde{M}_{11}) & & \tilde{F}_{L1N} - \omega^2 \tilde{M}_{N1} & & \\ & \ddots & & \ddots & \\ & & \tilde{F}_{LN1} - \omega^2 \tilde{M}_{1N} & & \\ & & & \bar{S}_N + \tilde{F}_{LNN} - \omega^2 (\bar{M}_N + \tilde{M}_{NN}) & \\ & & & & \end{bmatrix} \begin{bmatrix} \tilde{A}_1 \\ \vdots \\ \tilde{A}_N \end{bmatrix} = \begin{bmatrix} \tilde{F}_{ex1} \\ \vdots \\ \tilde{F}_{ex2} \end{bmatrix}$$

The case of internal forces can be solved by separating the body into several bodies tied by internal forces, with connection equations giving the unknown forces (for example, the beam of a catamaran).

2.3.9 Drift forces :

For a distribution of singularities kinematically equivalent to bodies oscillating in waves, we define the Kochin function by :

$$\tilde{H}(\theta) = -\frac{1}{4\pi \text{sh } m_0 h} \iint_{\Sigma} \left(\tilde{\sigma} + \tilde{\mu} \frac{\partial}{\partial n} \right) \text{ch } m_0 (z+h) e^{-im_0 (x' \cos \theta + y' \sin \theta)} dS(M')$$

with for a mixed distribution :

$$\tilde{\sigma} = \sum_{q=1}^6 \tilde{V}_{Ei} \cdot \bar{n} - \frac{\partial \tilde{\Phi}_I}{\partial n}; i = 1, 2, \dots, N$$

$$\tilde{\mu} = \tilde{\mu}_D + \sum_{i=1}^N \sum_{q=1}^6 \tilde{\mu}_{Ri} \cdot \tilde{A}_i^q$$

and for a source distribution :

$$\tilde{\sigma} = \tilde{\sigma}_D + \sum_{i=1}^N \sum_{q=1}^6 \tilde{\sigma}_{Ri} \cdot \tilde{A}_i^q$$

By application of the momentum equation, we obtain the Maruo-Newman formulas, which give two horizontal resultant drift forces and the vertical resultant drift moment exerted on all the bodies:

$$\langle F_x \rangle_y = -2\pi\rho\omega \left(\frac{\cos \beta}{\sin \beta} \right) \text{Im } \tilde{H}(\beta) - 2\pi\rho \frac{m_0 (k_0 h)^2}{h[(m_0 h)^2 - (k_0 h)^2 + k_0 h]} \int_0^{2\pi} [\tilde{H}(\theta)]^2 \left(\frac{\cos \theta}{\sin \theta} \right) d\theta$$

$$k_0 = \frac{\omega^2}{g}$$

and for the moment at a fixed point O (mooring) :

$$\langle M_z(O) \rangle = -2\pi\rho\omega \text{Re } \tilde{H}(\beta) - 2\pi\rho \frac{(k_0 h)^2}{h[(m_0 h)^2 - (k_0 h)^2 + k_0 h]} \int_0^{2\pi} \tilde{H}(\theta) \cdot \tilde{H}(\theta) d\theta$$

For a point O' moving with the bodies (dynamic positioning), we have :

$$\langle M_z(O') \rangle = \langle M_z(O) \rangle - \langle \tau_x \cdot F_{My} - \tau_y \cdot F_{Mx} \rangle$$

It can be demonstrated that, without external forces, the drift forces in the wave direction are positive :

$$\langle F_{\beta} \rangle = 2\pi\rho \frac{m_0(k_0h)^2}{h[(m_0h)^2 - (k_0h)^2 + k_0h]} \int_0^{2\pi} [H(\theta)]^2 [1 - \cos(\theta - \beta)] d\theta >= 0$$

The second method is the use of direct pressure integration at second order. It must be noticed that at second order, the average value of second order potential is zero, and the constant issue of Lagrange's equation F_2 is zero in infinite depth and also in finite depth for a freely floating body (not for a body artificially maintained at a constant height). The expression of average forces and moment at second order on the body number i is then given by :

$$\begin{bmatrix} \bar{F}_{Mi} \\ \bar{M}_{Mi} \end{bmatrix} = -\omega^2 \begin{bmatrix} \bar{P} & \bar{T} \\ -\bar{T} & \bar{I} \end{bmatrix} \begin{bmatrix} \bar{\tau}_i \\ \bar{\theta}_i \end{bmatrix}$$

$$\bar{F}_{deri} = \langle \bar{\theta}_i \wedge \bar{F}_{Mi} - [S_{33}(-\frac{\theta_{xi}^2 + \theta_{yi}^2}{2} z_F) + S_{34}(\frac{\theta_{yi} \cdot \theta_{zi}}{2}) + S_{35}(-\frac{\theta_{xi} \cdot \theta_{zi}}{2})] \cdot \bar{i}_z \rangle$$

$$+ \rho \iint_{\Sigma_i} [P_0 \bar{P} \cdot \text{grad} \frac{\partial \Phi}{\partial t} + \frac{1}{2} \rho (\text{grad} \Phi)^2 - F_2] \cdot \bar{n}_g dS - \frac{\rho g}{2} \int_{\Gamma_i} (\zeta - Z)^2 \cdot \bar{n}_g dS >$$

$$\bar{M}_{deri}(O') = \langle \bar{\theta}_i \wedge \bar{M}_{Mi}(O') - [S_{43}(-\frac{\theta_{xi}^2 + \theta_{yi}^2}{2} z_F) + S_{44}(\frac{\theta_{yi} \cdot \theta_{zi}}{2}) + S_{45}(-\frac{\theta_{xi} \cdot \theta_{zi}}{2})] \cdot \bar{i}_x \rangle$$

$$- [S_{53}(-\frac{\theta_{xi}^2 + \theta_{yi}^2}{2} z_F) + S_{54}(\frac{\theta_{yi} \cdot \theta_{zi}}{2}) + S_{55}(-\frac{\theta_{xi} \cdot \theta_{zi}}{2})] \cdot \bar{i}_y \rangle$$

$$+ \rho \iint_{\Sigma_i} [P_0 \bar{P} \cdot \text{grad} \frac{\partial \Phi}{\partial t} + \frac{1}{2} \rho (\text{grad} \Phi)^2 - F_2] \cdot \bar{n}_g dS - \frac{\rho g}{2} \int_{\Gamma_i} (\zeta - Z)^2 \cdot \bar{n}_g dS >$$

$$\zeta = -\frac{1}{g} \frac{\partial \Phi}{\partial t} \Big|_{z=0} : \text{wave height} ; Z = P_0 \bar{P} \cdot \bar{i}_z \Big|_{z=0} : \text{vertical displacement at free surface}$$

$\bar{n}_g = \bar{n}_0$ for the forces

$\bar{n}_g = O\bar{P}_0 \wedge \bar{n}_0$ for the moments around O' moving with the body and the transportation to a fixed point O is given by :

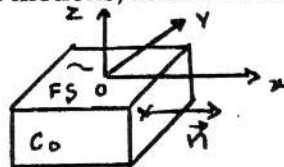
$$\langle \bar{M}_{deri}(O) \rangle = \langle \bar{M}_{deri}(O') \rangle + \langle \bar{\tau}_i \wedge \bar{F}_{Mi} \rangle$$

For a mixed distribution, the difficulty lays in the poor accuracy of velocity calculations for normal dipoles. To avoid this problem, we can solve one supplementary integral equation with a source distribution, once the motions are known, with one second member equal to the normal perturbation velocity of the bodies. The only benefit would be in the case of the calculation of motions by sources being wrong, which is not the case. The solution is then the same as with source distribution. In any cases, the calculation of second order forces with pressure integration requires the solution of at least one integral equation with sources.

2.5 Solution of the inner problem of oscillations in a tank:

2.5.1 The inner problem :

We consider a tank with forced motions, as shown on the figure below :



The governing equations of the inner and outer problems are [23] :

$$\left\{ \begin{array}{l} \text{Inner problem :} \\ \Delta\Phi = 0 \\ \left. \frac{\partial\Phi}{\partial n} \right|_{C_0} = -\bar{V}_E \cdot \bar{n}|_{C_0} \\ \left. \frac{\partial^2\Phi}{\partial t^2} + g \frac{\partial\Phi}{\partial z} \right|_{z=0} = -k_0\Phi + g \left. \frac{\partial\Phi}{\partial z} \right|_{z=0} = 0 \end{array} \right. \quad \left\{ \begin{array}{l} \text{Outer problem :} \\ \Delta\Phi = 0 \\ \left. \frac{\partial\Phi}{\partial n} \right|_{C_0} = \bar{V}_E \cdot \bar{n}|_{C_0} \\ \lim_{\epsilon' \rightarrow 0^+} \left(\frac{\partial^2\Phi}{\partial t^2} + 2\epsilon' \frac{\partial\Phi}{\partial t} + g \left. \frac{\partial\Phi}{\partial z} \right|_{z=0} \right) = 0 \end{array} \right.$$

$$\bar{V}_E = \bar{V}_E^* \cos \omega t$$

and :

$$-\bar{V}_E \cdot \bar{n} = -\omega \sin \omega t \left[\sum_{q=1}^3 A_i^q \bar{e}_q \cdot \bar{n} + \sum_{q=4}^6 A_i^q (\bar{e}_{q-3} \wedge O\bar{P}_0) \cdot \bar{n} \right]$$

In complex notation :

$$-\bar{V}_E \cdot \bar{n} = i\omega \left[\sum_{q=1}^3 A_i^q \bar{e}_q \cdot \bar{n} + \sum_{q=4}^6 A_i^q (\bar{e}_{q-3} \wedge O\bar{P}_0) \cdot \bar{n} \right]$$

For this problem, the condition at infinity does not exist, so the response has no phase shift with excitation. For an excitation in $\sin \omega t$, the response will be in $\sin \omega t$. and the elementary inner problems of radiation are :

$$\left\{ \begin{array}{l} \text{Inner problem :} \\ \Delta\Phi_q = 0 \\ \left. \frac{\partial\Phi_q}{\partial n} \right|_{C_0} = \begin{array}{ll} \bar{e}_q \cdot \bar{n} & q = 1, 2, 3 \\ \bar{e}_{q-3} \wedge O\bar{P}_0 & q = 4, 5, 6 \end{array} \\ -k_0\Phi_q + g \left. \frac{\partial\Phi_q}{\partial z} \right|_{z=0} = 0; k_0 = \frac{\omega^2}{g} \end{array} \right.$$

$$\Phi = -i\omega \sum_{q=1}^6 \Phi_q A_q$$

2.5.2 Solution by Rankine singularities method :

The elementary problem can be solved by a Rankine singularity method, with a mixed distribution of sources and normal dipoles, with M panels on the free surface and a total of N panels on the free surface and on the body. We have :

$$\sigma = -\frac{\partial\Phi}{\partial n}; \mu = \Phi$$

$$\sigma|_{C_0} = -\left. \frac{\partial\Phi}{\partial n} \right|_{C_0}; \sigma|_{SL} = -k_0\Phi = -k_0\mu|_{SL}$$

And the discretized integral equations are :

$$\sum_{j=1}^N \mu_j \bar{D}_{ij} = -\sum_{j=1}^N \sigma_j \bar{S}_{ij}; \mu_j \text{ unknowns}$$

with :

$$\begin{cases} \overline{D_{ij}} = D_{ij} & s_j \in C_0 \\ \overline{D_{ij}} = D_{ij} - k_0 S_{ij} & s_j \in SL \end{cases}$$

$$\begin{cases} \overline{S_{ij}} = S_{ij} & s_j \in C_0 \\ \overline{S_{ij}} = 0 & s_j \in SL \end{cases}$$

$$S_{ij} = -\frac{1}{4\pi} \iint_{s_j} \frac{1}{M_i M'} ds(M')$$

$$\begin{cases} D_{ij} = -\frac{1}{4\pi} \iint_{s_j} \frac{\partial}{\partial n_{M'}} \frac{1}{M_i M'} ds(M') \\ D_{ii} = -0.5 \end{cases}$$

$$\begin{cases} \sigma_j = \bar{e}_q \cdot \bar{n}_j & q = 1, 2, 3 \\ \sigma_j = (\bar{e}_{q-3} \wedge O\bar{P}_0) \cdot \bar{n}_j & q = 4, 5, 6 \end{cases}$$

In the case of heave motion, we have an analytical solution of the problem, which is very useful to verify the accuracy of the numerical solution.

$$\Phi_3 = z + \frac{1}{k_0}$$

2.5.3 Resonance frequencies :

With this method, we can have all resonance frequencies in one calculation. The matrix S_{ij} is $(N \times M)$, the matrix D_{ij} is $(N \times N)$, resonance frequencies are the solution of :

$$\text{Det}(S_{ij} - k_0 D_{ij}) = 0 \text{ or } \text{Det}(S_{ij} D_{ij}^{-1} - \frac{1}{k_0} I) = 0$$

The eigenvalues are λ_n :

$$\lambda_n = \frac{1}{k_0} = \frac{g}{\omega_n^2} \Rightarrow \omega_n = \sqrt{\frac{g}{\lambda_n}} ; T_n = 2\pi \sqrt{\frac{\lambda_n}{g}}$$

These resonance frequencies are different from the irregular frequencies of the outer problem.

2.5.4 Kelvin singularities :

The problem can also be solved by a Kelvin singularity method, with Green's function. The inner problem Green's function is the real part of the outer problem Green's function in infinite water depth. The integral equations are written on the body only (not on the free surface). The difference is that we have now an inner problem, so the discontinuity on the diagonal coefficient must be equal to -0.5 instead of 0.5 for the outer problem. The solution by Kelvin singularities can be used with source or mixed distribution. In the case of source distribution, the accuracy of the solution is poor. To obtain good results, we use the Galerkin method. The integral equation are written in one control point but the whole integral equation is integrated on the influenced panel. With this method, it can be demonstrated that the solution is the same for all singularity distributions. This is done numerically by numerical Gaussian integration on the influenced panel. Numerical tests show that 4 points are sufficient to have agreement between the Kelvin source method and all other methods for a given mesh of the body.

2.5.5 Forces exerted on the tank :

The external forces R_E exerted on the tank can be divided into two parts : a part is of type added mass M^0 and a part of type hydrostatic coefficient K^0 :

$$\bar{R}_E = \omega^2 \sum_{q=1}^6 A_q M_{pq}^0 + \sum_{q=1}^6 A_q K_{pq}^0$$

$$M_{pq}^0 = \rho \iint_{C_0} \Phi_q \frac{\partial \Phi_p}{\partial n} dS = -\rho \iint_{C_0} \mu_q \sigma_p dS$$

$$K_{pq}^0 = \begin{bmatrix} 0 & 0 & 0 & 0 & 0 & 0 \\ 0 & 0 & 0 & 0 & 0 & 0 \\ 0 & 0 & CS_{33} & CS_{34} & CS_{35} & 0 \\ 0 & 0 & CS_{43} & CS_{44} & CS_{45} & 0 \\ 0 & 0 & CS_{53} & CS_{54} & CS_{55} & 0 \\ 0 & 0 & 0 & 0 & 0 & 0 \end{bmatrix}$$

$$CS_{33} = \iint_{SL} dS$$

$$CS_{34} = CS_{43} = \iint_{SL} y dS$$

$$CS_{35} = CS_{53} = -\iint_{SL} x dS$$

$$CS_{44} = \iint_{SL} y^2 dS$$

$$CS_{45} = CS_{54} = -\iint_{SL} xy dS$$

$$CS_{55} = \iint_{SL} x^2 dS$$

The hydrostatic terms are of another sign than in the outer problem and there is no term concerning the difference between the elevation of the centre of gravity and the centre of the hull. These terms are of great importance in the problem of capsizing.

2.5.6 Coupling with the outer problem :

When there is a body with a tank inside it, the coupling of the two problems is made by the mechanical equation :

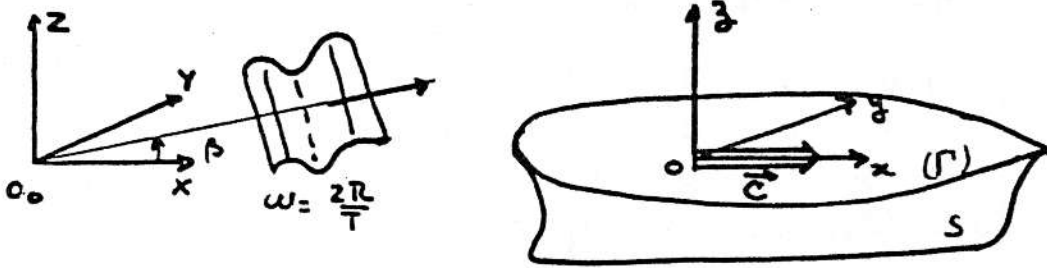
$$\sum_{q=1}^6 [-\omega^2 (\bar{M}_{pq} + \tilde{M}_{pq} + M_{pq}^0) + (\bar{S}_{pq} - K_{pq}^0)] \tilde{A}_q = \tilde{F}_{ex}^P$$

For several tanks, all the inner forces terms have to be added.

2.6 The problem with forward speed:

2.6.1 The problem in moving frame:

We consider first a fixed frame (O_0, X, Y, Z) and second frame which is a mean frame (O, x, y, z) , parallel to the first and moving with the ship velocity C ($X=x+Ct$), without oscillations, as shown on the figure below :



In the moving frame the potential of incident wave is :

$$\Phi_I = -\frac{ag \operatorname{ch} m_0(z+h)}{\omega \operatorname{ch} m_0 h} \cos [m_0(x \cos \beta + y \sin \beta) - \omega_e t]$$

with : $\omega^2 = gm_0 \operatorname{th} m_0 h$, and $\omega_e = \omega - Cm_0 \cos \beta$

ω_e is the encounter frequency.

2.6.2 The linearized problem :

In the moving frame, the linearized problem of seakeeping with forward speed can be written as follows, if we neglect the coupling terms with the problem of wave resistance, supposed to be of greater order [6] [7] [8] [13] :

$$\left\{ \begin{array}{l} \Delta \phi = 0 \\ \frac{\partial \phi}{\partial n} \Big|_{C_0} = \vec{V}_E \cdot \vec{n} \Big|_{C_0} \\ \frac{\partial^2 \phi}{\partial t^2} + 2\epsilon' \frac{\partial \phi}{\partial t} + g \frac{\partial \phi}{\partial z} - 2C \frac{\partial^2 \phi}{\partial t \partial x} - 2C\epsilon' \frac{\partial \phi}{\partial x} + C^2 \frac{\partial^2 \phi}{\partial x^2} \Big|_{z=0} = E\phi \Big|_{z=0} = 0 \\ \phi \rightarrow \phi_I \text{ at } \infty \end{array} \right.$$

The body condition is at first order coupled with the forward speed, supposed to be of order 0.

$$\frac{\partial \Phi}{\partial n} \Big|_{C_0} = \vec{V}_E \cdot \vec{n} \Big|_{C_0} = [C \cdot \vec{i}_x + (\vec{\tau} + \vec{\theta} \wedge O\vec{P}_0) + C(\vec{i}_x \wedge \vec{\theta})] \cdot \vec{n}_0$$

$\vec{\tau}$ and $\vec{\theta}$ are the translations and rotations at first order.

This coupling gives a modification of added mass and damping terms, due to the radiation potential which is now :

$$\tilde{\Phi}_R = -i\omega_e \sum_{q=1}^6 \tilde{A}_q \tilde{\Phi}_R^q - C\tilde{A}_6 \tilde{\Phi}_R^2 + C\tilde{A}_5 \tilde{\Phi}_R^3$$

The added mass and damping which were at zero speed :

$$\tilde{M}^{pq} = M^{pq} + \frac{i}{\omega_e} B^{pq}$$

$$M^{pq} = -\rho \iint_{C_0} \phi_R^{q*} \frac{\partial \phi_R^{p*}}{\partial n} dS, \quad B^{pq} = -\rho \omega \iint_{C_0} \phi_R^{q**} \frac{\partial \phi_R^{p*}}{\partial n} dS$$

become [6] [7] [13] :

$$\tilde{M}'^{p5} = \tilde{M}^{p5} + \frac{iC}{\omega_e} \tilde{M}^{p3}; \quad \tilde{M}'^{p6} = \tilde{M}^{p6} - \frac{iC}{\omega_e} \tilde{M}^{p2}$$

Diffraction forces are not modified, we have only to take into account that pressures are expressed in the moving frame :

$$p = -\rho \left(\frac{\partial \phi}{\partial t} - C \frac{\partial \phi}{\partial x} \right)$$

So we have now :

$$\tilde{M}^{pq} = -\rho \iint_{C_0} \left(\tilde{\Phi}_R^q - \frac{iC}{\omega_e} \frac{\partial \tilde{\Phi}_R^q}{\partial x} \right) \sigma_p dS$$

$$\text{with } \sigma_p = \begin{cases} \bar{e}_p \cdot \bar{n} & p = 1, 2, 3 \\ (\bar{e}_{p-3} \wedge O\bar{P}_0) \cdot \bar{n} & p = 4, 5, 6 \end{cases}$$

For the diffraction problem :

$$\tilde{F}_{ex}^p = -\rho \iint_{C_0} \left[-i\omega_e (\tilde{\Phi}_D + \tilde{\Phi}_I) - C \left(\frac{\partial \tilde{\Phi}_D}{\partial x} + \frac{\partial \tilde{\Phi}_I}{\partial x} \right) \right] \sigma_p dS$$

And for the motion equation :

$$\sum_{q=1}^6 [-\omega_e^2 (\bar{M}_{pq} + \tilde{M}_{pq}) + \bar{S}_{pq}] \tilde{A}_q = \tilde{F}_{ex}^p$$

After calculations of the amplitude of motions at encounter frequency ω_e , second order forces are obtained by pressure integration at second order in the moving frame [14]. In the fixed frame, we have :

$$\vec{F}_{hd2} = \langle \vec{F}_{hs2} + \theta \wedge \vec{F}_{hd1} + \rho \iint_{C_0} \left[\frac{1}{2} (\text{grad } \phi)^2 + P_0 P \text{ grad } \frac{\partial \phi}{\partial t} \right] \vec{n}_g dS - \frac{\rho g}{2} \int_{\Gamma_0} (\zeta - Z)^2 \vec{n}_g dS \rangle$$

F_{hs2} being the hydrostatic forces at second order, F_{hd1} the hydrodynamic force at first order, C_0 the hull and Γ_0 the waterline at rest.

The only supplementary approximation is to neglect the second order derivatives of the space variables in factor of C coming from the derivation of the gradient in the moving frame.

2.6.3 The approximations of the linearized problem :

The exact linearized free surface condition is given by :

$$\lim_{\epsilon' \rightarrow 0^+} \left. \frac{\partial^2 \Phi}{\partial t^2} + 2\epsilon' \frac{\partial \Phi}{\partial t} + g \frac{\partial \Phi}{\partial z} - 2C \frac{\partial^2 \Phi}{\partial t \partial x} - 2C\epsilon' \frac{\partial \Phi}{\partial x} + C^2 \frac{\partial^2 \Phi}{\partial x^2} \right|_{z=0} = 0 \quad (1)$$

$$\text{-----} \quad (2)$$

$$\text{-----} \quad (3)$$

The exact linearized free surface condition [7] [10] is given by (1). The first approximation consists in neglecting the term in C^2 in this equation [8] [9] (2) and the second [13] (3) to neglect all the terms in C and C^2 , which give the free surface condition without forward speed at the encounter frequency ω_e . This approximation is the one used in the slender ship theory [4].

The computation code using these approximations are called respectively DYNAPLOUS (Bougis 1980)(1), ARGOS (Grékas 1981)(2), AQUAPLUS (Delhommeau 1988)(3). All distributions are source distributions, the free surface condition being satisfied by a Green's function. In the case of DYNAPLOUS, this function is singular for a value of the non dimensional parameter $\tau = \omega_e C/g = 1/4$. For ARGOS, there is no singularity for $\tau = 1/4$, but the Green's function is divergent for $\tau > 1/2$. In these two cases, the Green's function is computed by numerical integration with 10 to 50 integration points, depending of the period. The approximation AQUAPLUS has no singularity and is computed by numerical interpolation as in the case of zero forward speed.

2.6.4 The Green's functions in infinite water depth:

In infinite water depth, the expressions of the Green's function for the three approximations are given by:

$$G = \text{Re } \tilde{G} e^{-i\omega t}$$

DYNAPLOUS:

$$\tilde{G} = -\frac{1}{4\pi} \left[\frac{1}{MM'} - \frac{1}{MM_1} \right] + \tilde{\varphi}; M'(x', y', z'); M_1'(x', y', -z')$$

$$\tilde{\varphi} = \frac{g}{4\pi^2} \int_{-\pi}^{+\pi} d\theta \int_0^{\infty} \frac{e^{k(z+z'+i\omega)}}{(kC \cos \theta + \omega_e)^2 + 2i\epsilon'(kC \cos \theta + \omega_e) - gk} k dk$$

4 real poles + singularity at $\tau = \frac{1}{4}$

ARGOS:

$$\tilde{G} = -\frac{1}{4\pi} \left[\frac{1}{MM'} - \frac{1}{MM_1} \right] + \tilde{\varphi}; M'(x', y', z'); M_1'(x', y', -z')$$

$$\tilde{\varphi} = \frac{g}{4\pi^2} \int_{-\pi}^{+\pi} d\theta \int_0^{\infty} \frac{e^{k(z+z'+i\omega)}}{2kC \cos \theta + \omega_e^2 + 2i\epsilon'(kC \cos \theta + \omega_e) - gk} k dk$$

2 real poles + divergence for $\tau > \frac{1}{2}$

AQUAPLUS:

$$\tilde{G} = -\frac{1}{4\pi} \left[\frac{1}{MM'} - \frac{1}{MM_1} \right] + \tilde{\varphi}; M'(x', y', z'); M_1(x', y', -z')$$

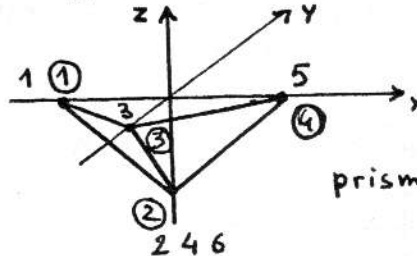
$$\tilde{\varphi} = \frac{g}{4\pi^2} \int_{-\pi}^{+\pi} d\theta \int_0^{\infty} \frac{e^{k(z+z'+i\omega)} k dk}{\omega_e^2 + 2ie'\omega_e - gk}$$

1 real pole independant from θ + symmetry of revolution

III - DESCRIPTION OF THE COMPUTER CODES :

After this brief presentation of the main equations used in the linear theory of seakeeping, we will now describe the computer codes allowing us to solve these problems. The described codes will be AQUADYN 2.1, CUVE and AQUAPLUS. All these codes can use one symmetry plane, which is arbitrarily set as xOz, so only half of the body at $y > 0$ or < 0 has to be meshed. The panels constituting a body must be arranged so that the normal at a panel is directed outside. There are two way of describing the mesh of a body. The first is historically the Hess and Smith type. In this case, we enter the number of the point, the number of the opposite point on the panel and the coordinates (I, M(I), X, Y, Z). The panels and the outside normal are built by I, I+1, M(I); M(I)-1. If there is no opposite point on the panel, M(I)=0. The mesh is described by rows and is generally easy to build for ship hulls, but very complicated for complex hulls, like a semi-submersible platform. We prefer to use the natural type of data, where we enter the number of the point and his coordinates (I, X, Y, Z) and after having entered all the points, the number of the points (M1, M2, M3, M4) defining the panel and the outside normal. This method is more simple as the previous one, but has to be verify by graphical output, because each panel can have a wrong normal, which is not the case when the body is described by rows.

Example of the two kind of data is given below:



Hess and Smith data :

1	1			
1	4	-1.	0.	0.
2	0	0.	0.	-1.
3	6	0.	-1.	0.
4	0	0.	0.	-1.
5	0	1.	0.	0.
6	0	0.	0.	-1.
0	0	0.	0.	0.

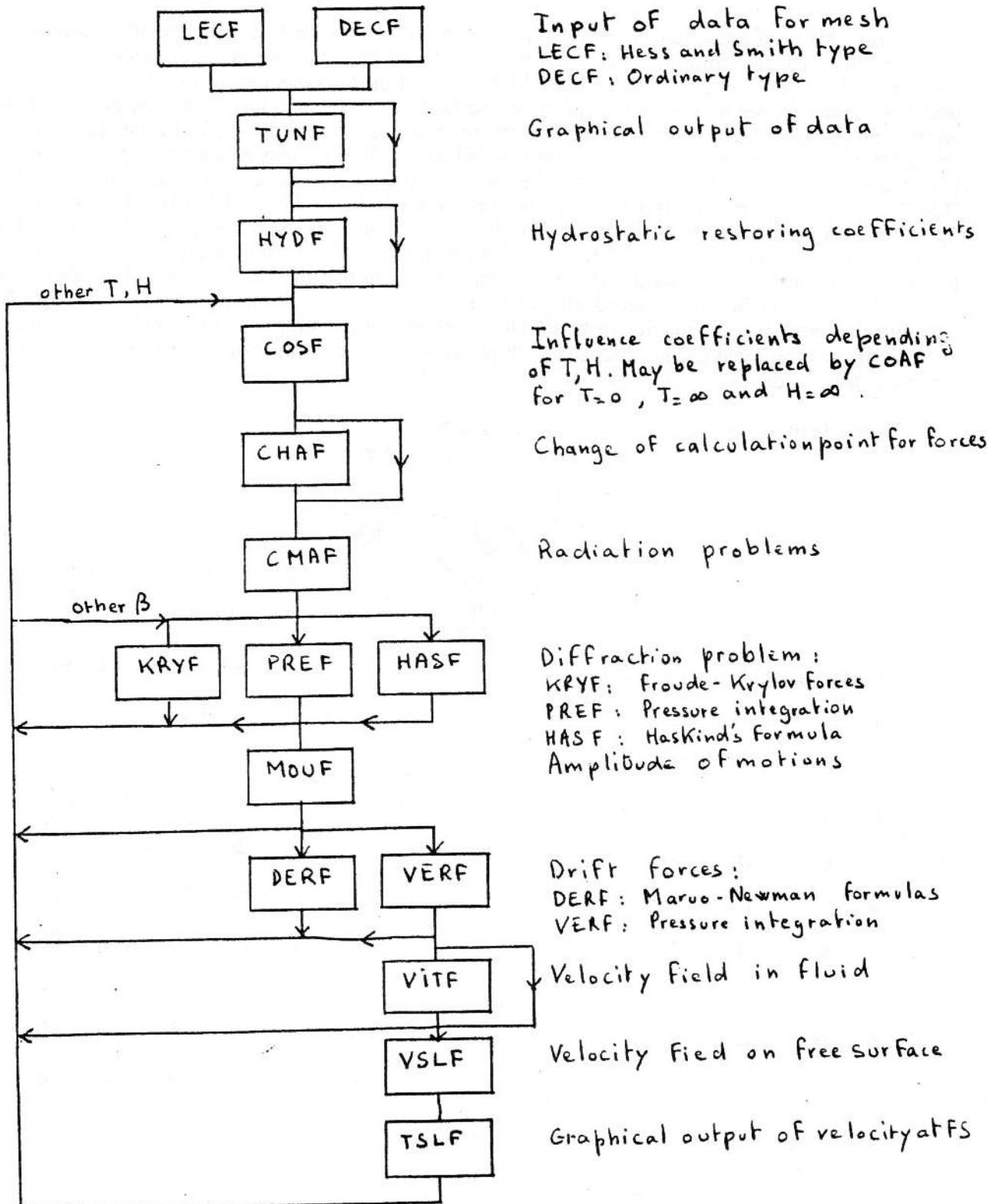
Natural data : (n)

2	1			
1	-1.	0.	0.	
2	0.	0.	-1.	
3	0.	-1.	0.	
4	1.	0.	0.	
0	0.	0.	0.	
1	2	3	1	
3	2	4	3	
0	0	0	0	

3.1 AQUADYN 2.1:

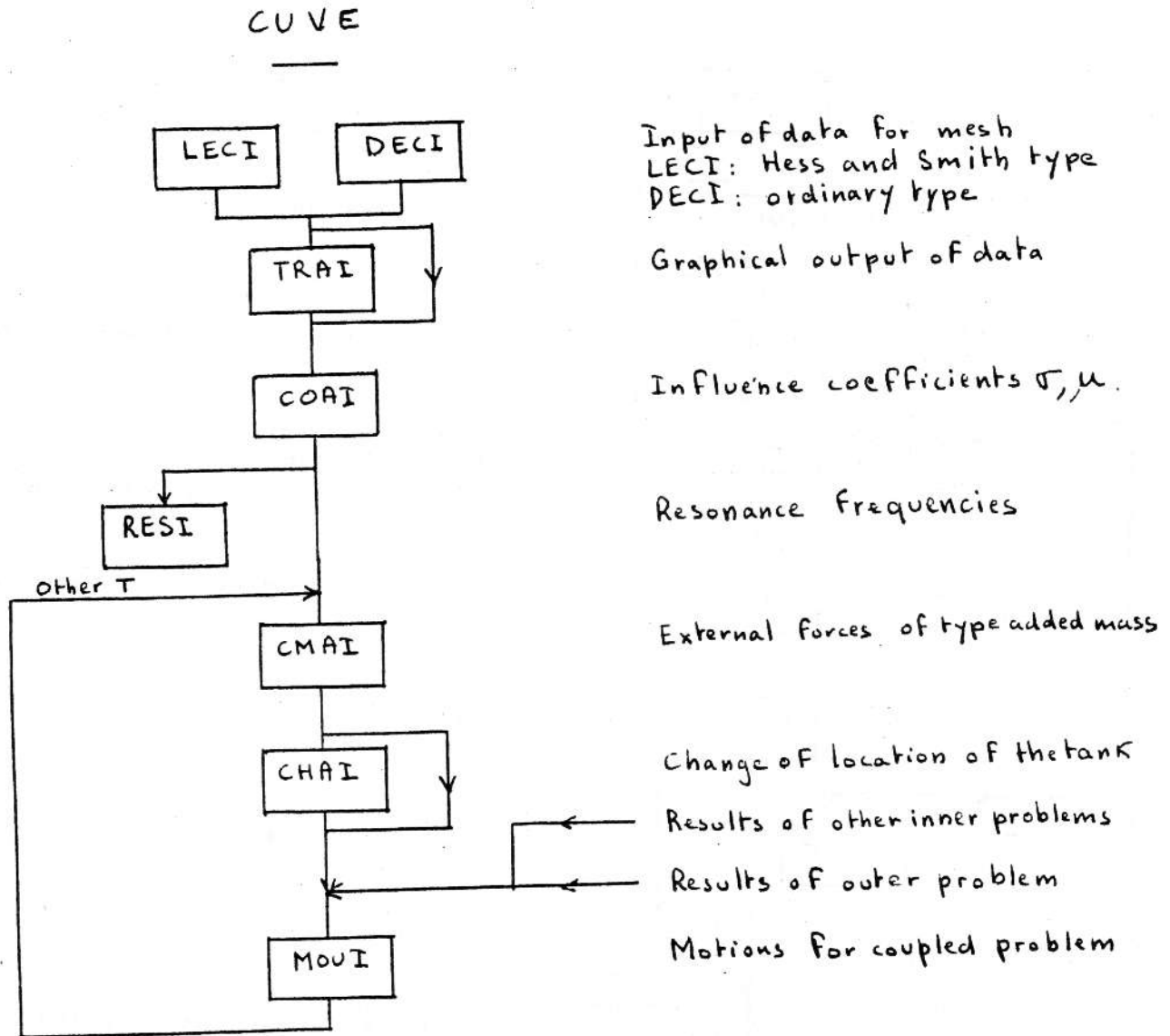
AQUADYN 2.1 is a series of principal programs, communicating by sequential files. All the names are ended by F. Complex linear systems are solved in CMAF, PREF, VERF. The names of the programs and their function are described below:

AQUADYN 2.1



3.2 CUVE :

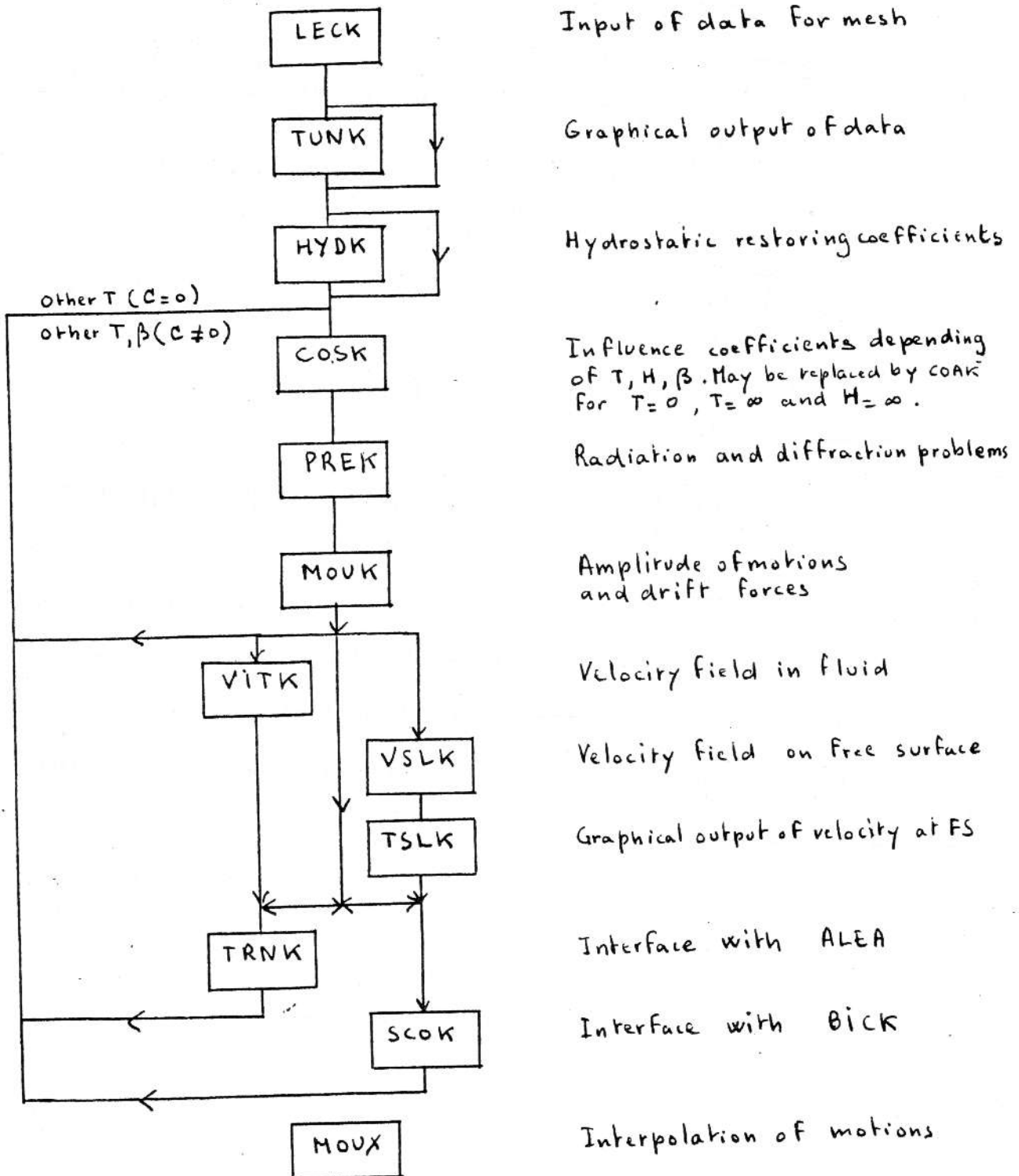
Like AQUADYN 2.1, CUVE is a series of principal programs, communicating by sequential files. All the names are ended by I. This program can be used to obtain only the resonance frequencies of tanks. For the coupled problem, the results of each calculation is kept in direct access file. The results of all tanks calculations and outer problem are gathered at the beginning of the program allowing us to compute motions. The names of programs and their function are given below :



3.3 AQUAPLUS :

AQUAPLUS is also a series of principal programs, but communicating by direct access files. All the names are ended by K. In this code, the calculation are made by series (calculation with the same configuration but with different periods). Only one complex linear system is solved in PREK (all directions of waves are entered in COSK for $C=0$). The results of each series are kept for further calculations (complementary calculations with AQUAPLUS or statistical exploitation on irregular seas by code ALEA or calculation of slow drift motions by code BICK). The names of programs and their function are given below :

AQUAPLUS



IV - NUMERICAL RESULTS AND APPLICATIONS:

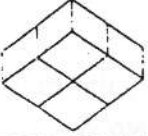
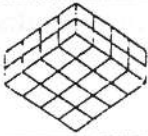
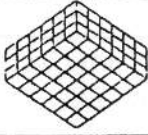
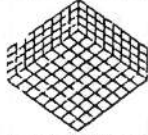
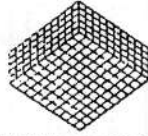
Since 1978, these codes have been widely used for many purposes [19] [20] [21] [23] [24] and for several international tests [26] [27] [28] [29]. So we will present here only significant examples of the behaviour of the codes. All the figures are gathered at the end of the paragraph.

4.1 Barge D.N.V., Influence of mesh refinement:

The first test is the D.N.V. barge used for comparison of computer codes in 1977. The body is a parallelepipedic barge of 90 m length, 90 m of breadth with a draft of 40 m. The inertia are:

$I_{44}=3.5369 \text{ E11 kgxm}^2$, $I_{55}=3.33649 \text{ E11 kgxm}^2$, $I_{66}=3.5113 \text{ E11 kgxm}^2$. The calculation point is at gravity centre located at $z=-10.62 \text{ m}$.

The results are presented on the figures 1 to 12 for different mesh. The table below show the mesh and the number of panels per wave length at different periods.

Périod (s)	6	10	15	20	25	30
	1,2	3,4	7,8	13,8	21,6	31,2
	2,5	6,9	15,6	27,7	43,3	62,4
	3,7	10,4	23,4	41,6	65	93,6
	5	13,8	31,2	55,4	86,6	124,8
	6,2	17,3	39	69,3	108	156

The coefficients for added mass and damping coefficients are:

$$CM_{11} = \frac{M_{11}}{\rho L^3}, CM_{33} = \frac{M_{33}}{\rho L^3}, CA_{11} = \frac{B_{11}}{\rho \omega L^3}, CA_{33} = \frac{M_{33}}{\rho \omega L^3}$$

The points at 1 s and 40 s are obtained by the asymptotic formulations for $T=0$ and $T=\infty$. It can be seen that a minimum of 54 panels is needed to obtain a beginning of convergence of the results. The behaviour for CA_{33} is not satisfying at $T=9$ s for certain mesh. The influence of mesh on exciting forces are less important than for the added mass and especially damping coefficients, because the diffraction problem is in a great part due to Froude-Krylov forces, which are the same for all mesh. At resonance of pitch motion, the influence of pitch motion on the other motions is sensitive. The drift forces by the two formulations are in good agreement for $T > 10$ s.

4.2 Irregular frequencies:

On figure 13, we can see the behaviour of CA33 between 8.7 s and 10 s. This behaviour is typical of an irregular frequency, which is theoretically located at 8.857 s. On figure 14, we see the elimination of this irregular frequency with a mixed distribution and with a source distribution. For the mixed distribution, the elimination is done by writing the condition of zero potential inside the hull on the normal of waterline panels at a distance of half height of the panel. The linear system are then solved by a least square method using unitary transformation of Householder type. For the source distribution, the free surface has been meshed with 4 panels and the condition written on these panels is that the normal derivative is zero.

4.3 Trawlers:

The figures 15, 16 and 17 show the mesh of three trawlers and the numerical results for heave and pitch compared with trials in wave tank. It can be seen that the calculations are in good agreement with experiments. On figures 16 and 17, we see the typical behaviour in heave of multihull in waves for 2 to 3 s. The mesh has to be refined for calculations at these periods.

4.3 Sphere:

The next test is for a floating hemisphere of radius $R=1$ m, with a regular mesh of N_θ on a half parallel and N_ψ on a half meridian, the total number of panels being $2N_\theta N_\psi$. The table below shows the comparison of numerical results for different mesh with the analytical results for a period of 1.59 s.

			Mouvements		Forces de dérive (second ordre)				
N_θ	N_ψ	N	$\frac{X}{a}$ m/m	$\frac{Z}{a}$ m/m	Mar.New $\frac{F_x}{a^2}$ N/m ²	Press. $\frac{F_x}{a^2}$ N/m ²	Press. $\frac{F_z}{a^2}$ N/m ²	Press. $\frac{M_y}{a^2}$ Nxm/m ²	
T = 1,59 s	12	12	288	0,311	0,407	6,34E3	6,24E3	-4,11E3	2,74E1
	12	10	192	0,310	0,413	6,33E3	6,28E3	-4,07E3	2,46E1
	10	10	200	0,312	0,411	6,32E3	6,18E3	-4,08E3	3,94E1
	10	6	120	0,310	0,423	6,30E3	6,22E3	-4,03E3	3,39E1
	8	8	128	0,313	0,418	6,28E3	6,10E3	-4,04E3	6,16E1
	8	5	96	0,312	0,427	6,27E3	6,13E3	-4,00E3	5,79E1
	6	6	72	0,316	0,434	6,21E3	5,92E3	-3,92E3	1,09E2
	6	4	48	0,313	0,460	6,20E3	5,96E3	-3,84E3	9,97E1
	5	3	30	0,314	0,508	6,16E3	5,83E3	-3,64E3	-1,40E2
	4	2	16	0,313	0,660	6,21E3	5,61E3	-2,75E3	2,10E2

Valeurs théoriques _____

0,40	6,28E3	6,28E3	-4,22E3	0
------	--------	--------	---------	---

In this table, we can see that the Maruo-Newman formulation is more stable than the pressure integration and that the results are in good agreement with the analytical results.

4.5 Pontoon :

The next example concerns the mesh of a deeply immersed body, without free surface effect. This is the case of the pontoons of a tension leg platform calculated by C. Berhaut. The figure 18 shows the 3 different meshes of this pontoon, with 1, 3 and 5 panels on each side. Figure 19 shows the results. We can deduce that a minimum number of 3 panels on each side is needed for convergence of terms in $1/R$.

4.6 Cylinder in finite depth :

The next case is the cylinder in finite depth. The mesh is 6 panels in vertical direction and 8 panels on the half horizontal part on the cylinder. For this case, we have theoretical results by the formula:

$$F = F^* \cos \omega\tau + F^{**} \sin \omega\tau$$

$$CF_1^* = \frac{F^*}{4\rho g R h a} = -\frac{2h}{R} \frac{\text{th } M_0}{M_0^2} \frac{Y_0(M_0 \frac{R}{h}) - Y_2(M_0 \frac{R}{h})}{[J_0(M_0 \frac{R}{h}) - J_2(M_0 \frac{R}{h})]^2 + [Y_0(M_0 \frac{R}{h}) - Y_2(M_0 \frac{R}{h})]^2}$$

$$CF_1^{**} = \frac{F^{**}}{4\rho g R h a} = -\frac{2h}{R} \frac{\text{th } M_0}{M_0^2} \frac{J_0(M_0 \frac{R}{h}) - J_2(M_0 \frac{R}{h})}{[J_0(M_0 \frac{R}{h}) - J_2(M_0 \frac{R}{h})]^2 + [Y_0(M_0 \frac{R}{h}) - Y_2(M_0 \frac{R}{h})]^2}$$

R being the radius, h the depth, $m_0 \text{th } m_0 h = k_0$, $k_0 = \omega^2/g$, $M_0 = m_0 h$, $K = k_0 h$.

J_0 and J_2 are the first kind Bessel functions of order 0 and 2 and Y_0 and Y_2 are the second kind Bessel functions of order 0 and 2. The results of AQUADYN and AQUADYN 2.1 compared with analytical results are presented on the figure 20. The agreement is very good, except at wave numbers greater than 4, where the mesh is too rough. With more panels, the agreement will be better.

4.7 Semi-submersible platform and tension leg platform:

The results presented on figures 21 and 22 are extracted from the I.T.T.C and I.S.S.C comparisons [27] [28].

4.8 T.P.S., second order calculations:

Here, we compare the Maruo-Newman formulation [14] to the pressure integration. The hull is a T.P.S (Turret Moored Production Ship) proposed as test at the Workshop of Bergen (1989)[29] The main dimension of the hull are: length = 230 m, breadth = 41 m, draft = 15 m. Computations have been made for several mesh differing only around the edge at the bottom of the hull as indicated on figure 23. Transfer function for drift forces, adimensioned by $\rho g L$ with $L = 41$ m and computed by the two formulations has been projected on the incident wave direction, which makes a 10 degree angle with the axis of the hull. The resulting force has to be positive. For more legibility, the forces issued of Maruo-Newman formulation have been shifted vertically of 0.2.

The results obtained with different mesh with Maruo-Newman formulation are in good agreement up to 0.55 rd/s. For $0.3 \text{ rd/s} < \omega < 0.5 \text{ rd/s}$, difference between the two formulations decrease when we refine the mesh around the edge and is negligible if there is no sharp angle. For rough mesh, the forces calculated by pressure integration are strongly negative. Influence of the depth of the corner is important on this anomaly which occurs when there is sharp angle near the free surface. This problem has already been studied by O. Faltinsen [15]. The agreement between the two formulations is a criterion of the quality of the results. The same phenomenon occurs for the calculation of second order slow drift forces.

Another possibility of discrepancy is the size of the panels. Calculations have been made on a spheroid fully immersed (length = 230 m, breadth = 41 m, radius = 15 m, immersion of the axis = 20 m). Two mesh have been done (396 and 792 panels) for which we have more than 12 panels per wave length for pulsations respectively lower than 0.67 and 0.95 rd/s. We see that for this body without sharp corners the difference between the two mesh is lower than 0.05 for more than 12 panels per wave length. It can be noticed that for a floating half spheroid, agreement between the two formulations is still better.

A mesh with 12 panels per wave length is sufficient for calculations at second order but some care on the mesh around sharp angles near the free surface have to be taken.

4.9 D.N.V. tank, inner problem :

The tank is a D.N.V. tank (90*90*40) filled with water. The tank has been meshed with 4 panels in the vertical direction and 8 panels in the horizontal direction, as on the free surface. The mesh is shown below. The table under show the resonance frequencies of all the motions of the hull. The greatest period in heave (564 s) is not a resonance period but is the consequence of the discretization.

FREQUENCES DE RESONANCES POUR LE(S) MOUVEMENT(S) DE :

PILONNEMENT		HEAVE	CAVALEMENT, TANGAGE		SURGE, PITCH
PERIODE :	1 =	564.879 S	PERIODE :	1 =	11.308 S
PERIODE :	2 =	7.500 S	PERIODE :	2 =	7.035 S
PERIODE :	3 =	6.219 S	PERIODE :	3 =	6.064 S
PERIODE :	4 =	3.672 S	PERIODE :	4 =	5.489 S
PERIODE :	5 =	4.298 S	PERIODE :	5 =	5.117 S
PERIODE :	6 =	4.758 S	PERIODE :	6 =	3.360 S
PERIODE :	7 =	5.006 S	PERIODE :	7 =	4.137 S
PERIODE :	8 =	5.389 S	PERIODE :	8 =	4.589 S
PERIODE :	9 =	2.230 S	PERIODE :	9 =	3.730 S

FREQUENCES DE RESONANCES POUR LE(S) MOUVEMENT(S) DE :

LACET		YAW	EMBARDEE, ROULIS		SWAY, ROLL
PERIODE :	1 =	9.056 S	PERIODE :	1 =	11.308 S
PERIODE :	2 =	5.868 S	PERIODE :	2 =	7.035 S
PERIODE :	3 =	5.027 S	PERIODE :	3 =	0.001 S
PERIODE :	4 =	3.325 S	PERIODE :	4 =	6.063 S
PERIODE :	5 =	4.635 S	PERIODE :	5 =	5.472 S
PERIODE :	6 =	3.528 S	PERIODE :	6 =	3.353 S
PERIODE :	7 =	4.273 S	PERIODE :	7 =	3.627 S
PERIODE :	8 =	3.802 S	PERIODE :	8 =	4.533 S
PERIODE :	9 =	5.751 S	PERIODE :	9 =	4.922 S

4.10 Barge D.N.V., influence of adimensional parameter τ :

The results obtained with the barge D.N.V. (90*90*40) in front wave at a Froude number of 0.15 are given on figures 24 and 25. The hull is meshed with 54 panels on the described part of the hull. The results of different approximations of free surface condition for hydrodynamic forces, motions and added resistance are shown. The parameter τ decreases when the period increases. The critical value of $\tau = 1/4$ is approximately at a period of 14 second. With the version of the codes used, the computing time for all the periods is 2 h 30 min for DYNAPLOUS, 15 min for ARGOS and 1 min for AQUAPLUS. At little τ , we see that the three approximations are very close, except for surge motion at 20 second where there is coupling with a resonance of pitch motion. The code DYNAPLOUS has a singular behaviour near the critical value of τ . At great values of τ the results diverge.

4.11 A practical case. Series 60 :

The second calculation with forward speed is for cargo hull of type Series 60. Computations have been made by AQUAPLUS at periods between 8 and 20 second in front waves for Froude numbers of 0.28; 0.22; 0.17, with blocks coefficients of 0.60; 0.70; 0.80. For front waves, the wave period for the critical value of τ in the fixed axis is given by :

$$T_C = 4 \pi C / (\sqrt{2} - 1)g = 3,09 C$$

where T_C is the wave period in the fixed axis and C the forward speed. For a hull of length $L = 193.5$ m, this formula gives : $T_C = 37.8$ s for $C = 12.21$ m/s, $T_C = 29.6$ s pour $C = 9.58$ m/s, and $T_C = 22.0$ s for $C = 7.12$ m/s.

For all periods, we have $\tau > 1/4$. Results are compared with those of the strip theory given in dotted line on the three first curves of figure 26 [4].

The AQUAPLUS results are close to those of the strip theory. In all cases, the location of the peak of added resistance is correctly evaluated, but its amplitude is over-evaluated. The results are better for high block coefficients and low speed. Unfortunately, experimental results are obtained with these two parameters varying simultaneously, which prevents all interpretation.

In [4], experimental results for heave and pitch motions show that the peak of added resistance is located at a resonance of the motions. A simplified theory of added resistance gives a resistance proportional to the square of amplitude of motions of heave and pitch, multiplied by their damping coefficient [1]. These motions are widely over evaluated by calculations. If we know the experimental values of the maximum, we can deduce a linear damping coefficient allowing us to respect the amplitude of motions at resonance. Computing the added resistance with these motions gives a good agreement with experiments as it can be seen on the last curve of figure 26.

4.12 Influence of damping on Beukelman cylinders :

To confirm this fact, we compute the added resistance of a prismatic hull (rectangular cylinder) of length 2.5 m, breadth 0.25 m and draft 0.25 m. This hull has been computed by W. Beukelman with the strip theory and results compared with experiments [11]. For a Froude number of 0.16, computations have been made by AQUAPLUS and DYNAPLOUS. Agreement is good. In this case, if we take a linear damping coefficient allowing us to give a good amplitude of motions at resonance, there is a good agreement on added resistance. For other calculations at a Froude number of 0.26 with the same damping coefficient, agreement is not so good, which can mean that damping is not entirely linear. For a prismatic hull of triangular section, motions and consequently added resistance are correctly computed without adding linear damping. Results are given on figures 27 and 28.

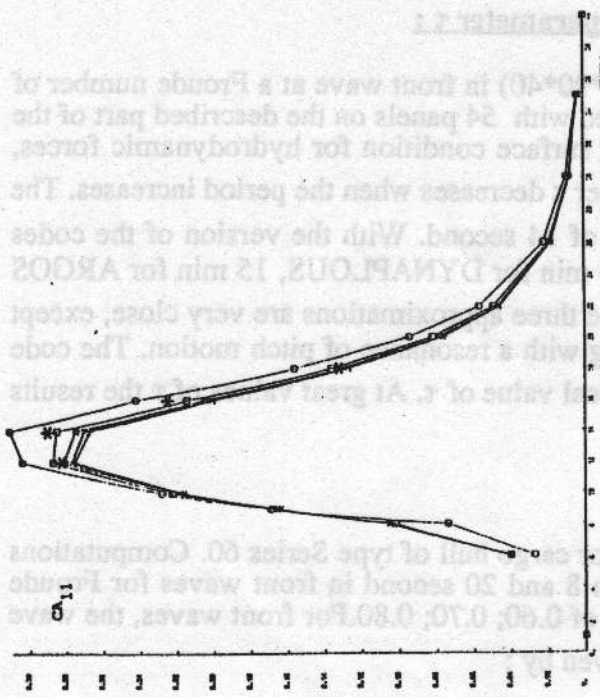


Figure 3

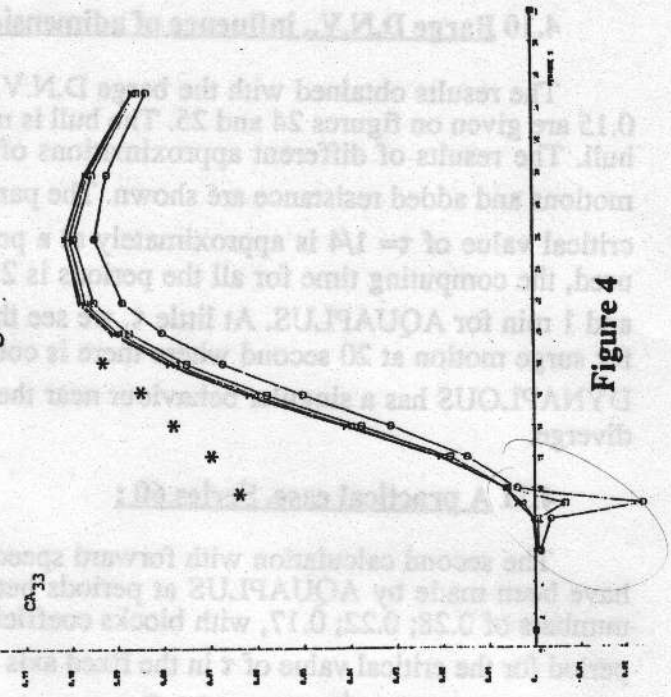


Figure 4

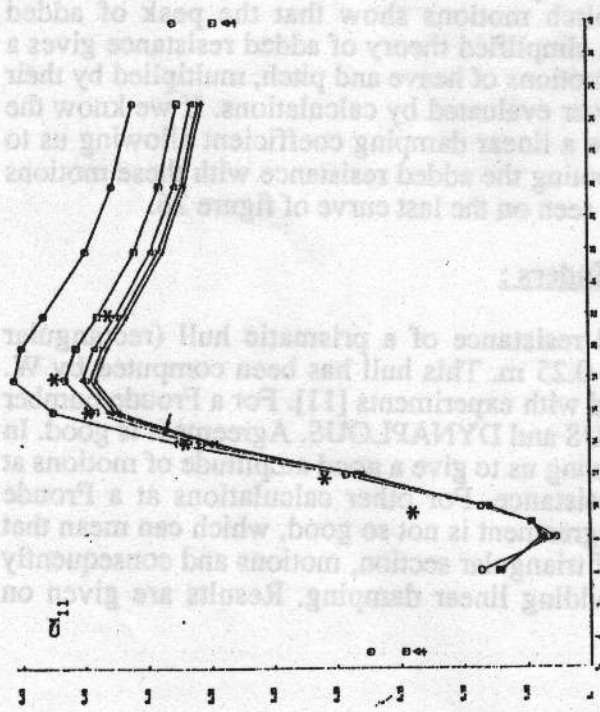
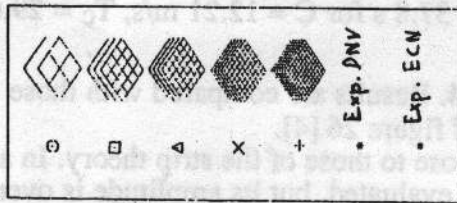


Figure 1

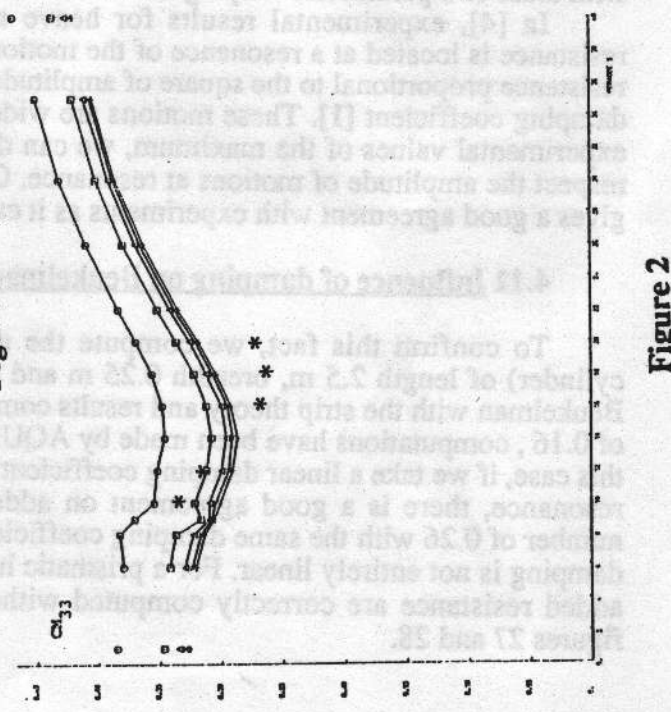


Figure 2

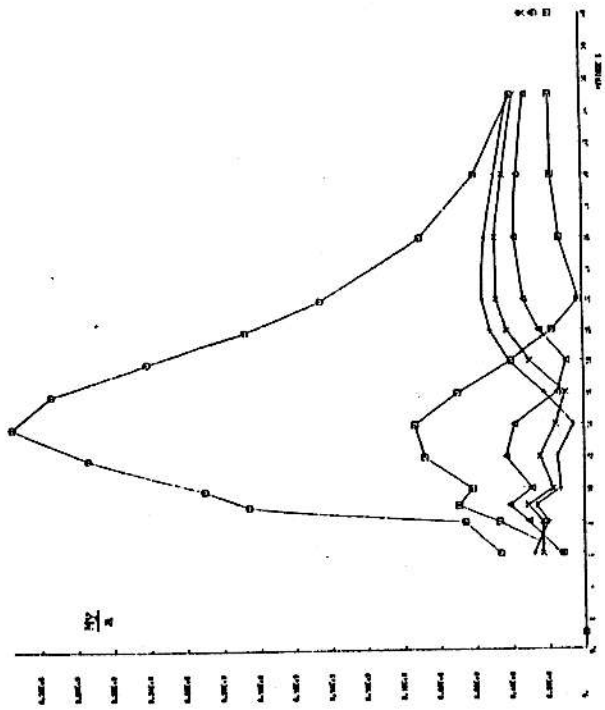


Figure 5

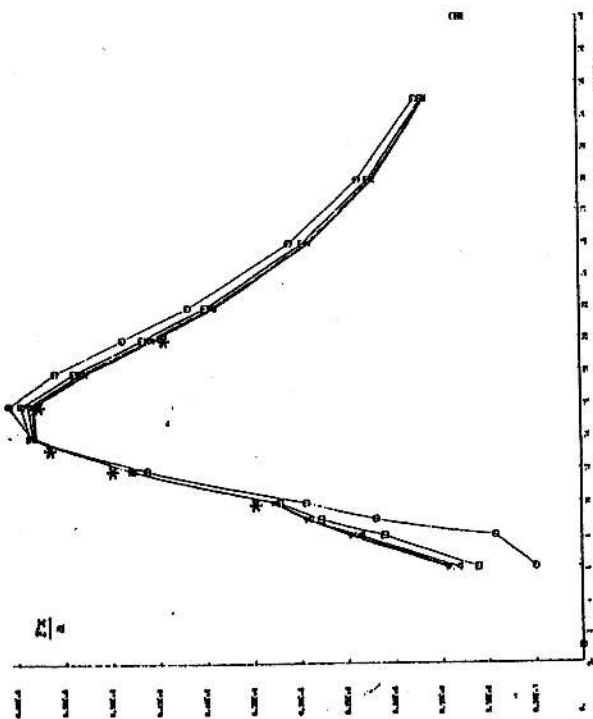
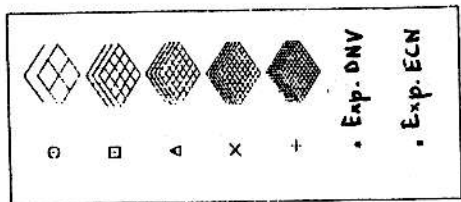


Figure 6

Figure 7

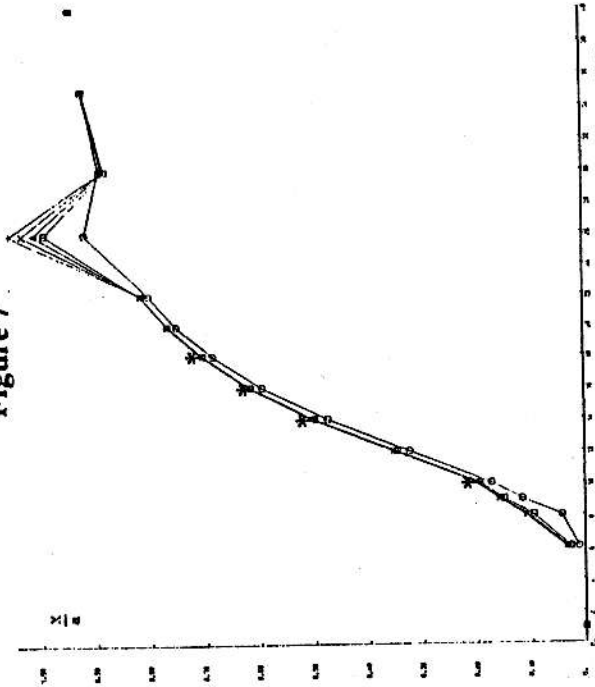


Figure 8

Figure 8

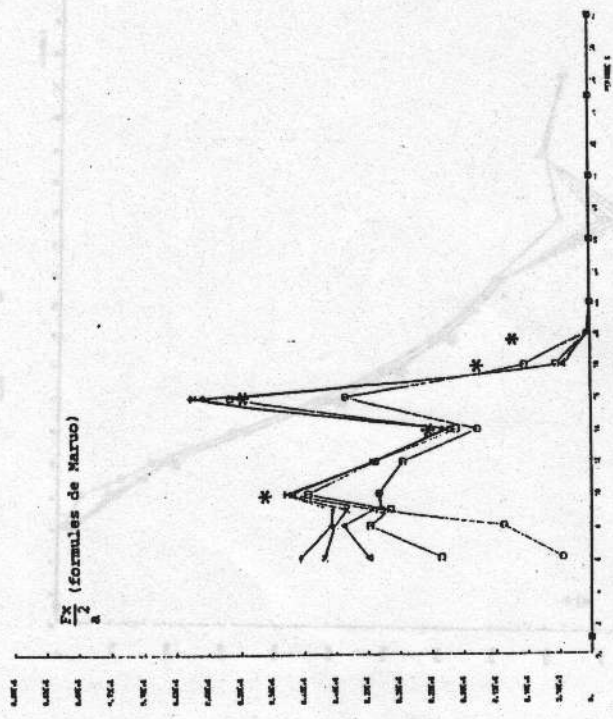


Figure 11

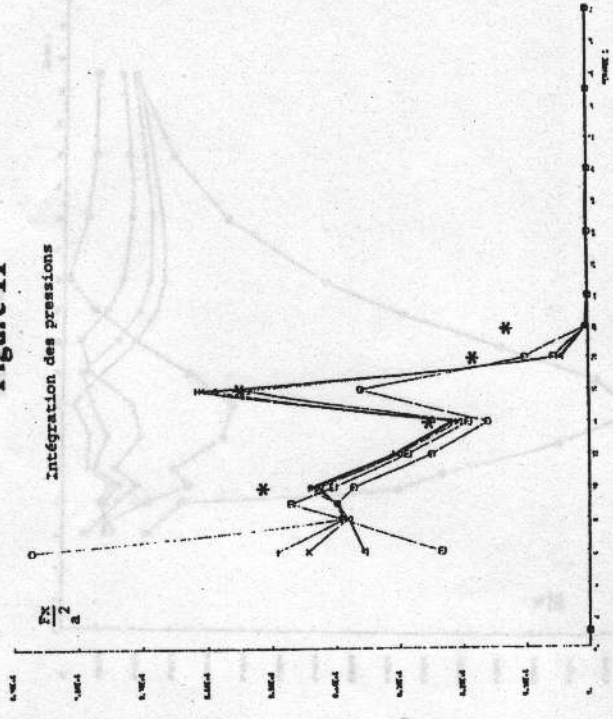


Figure 12

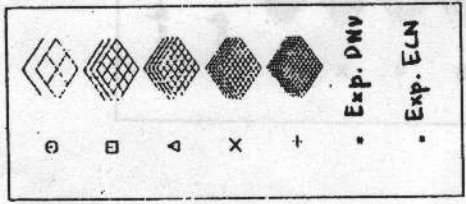


Figure 9

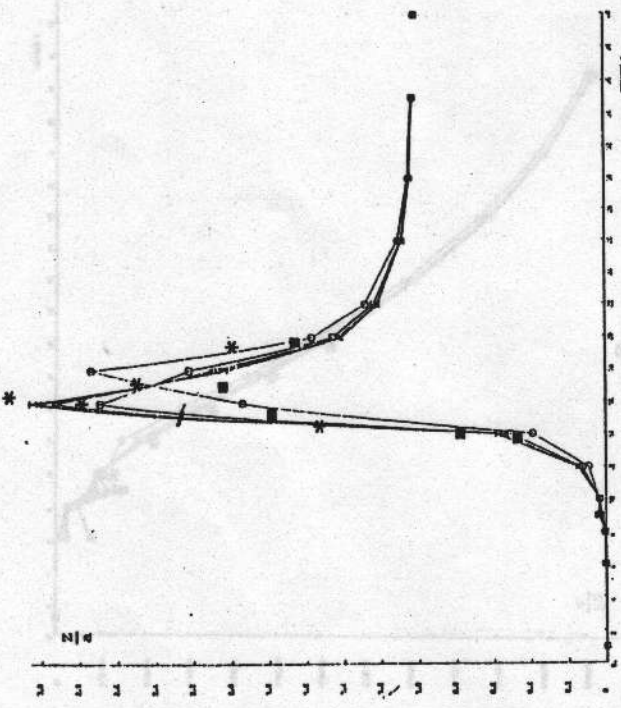


Figure 10

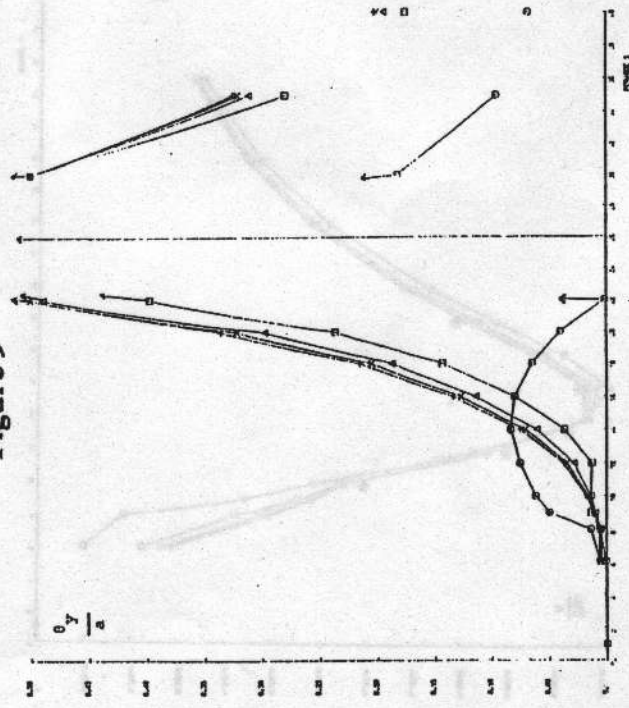


Figure 10

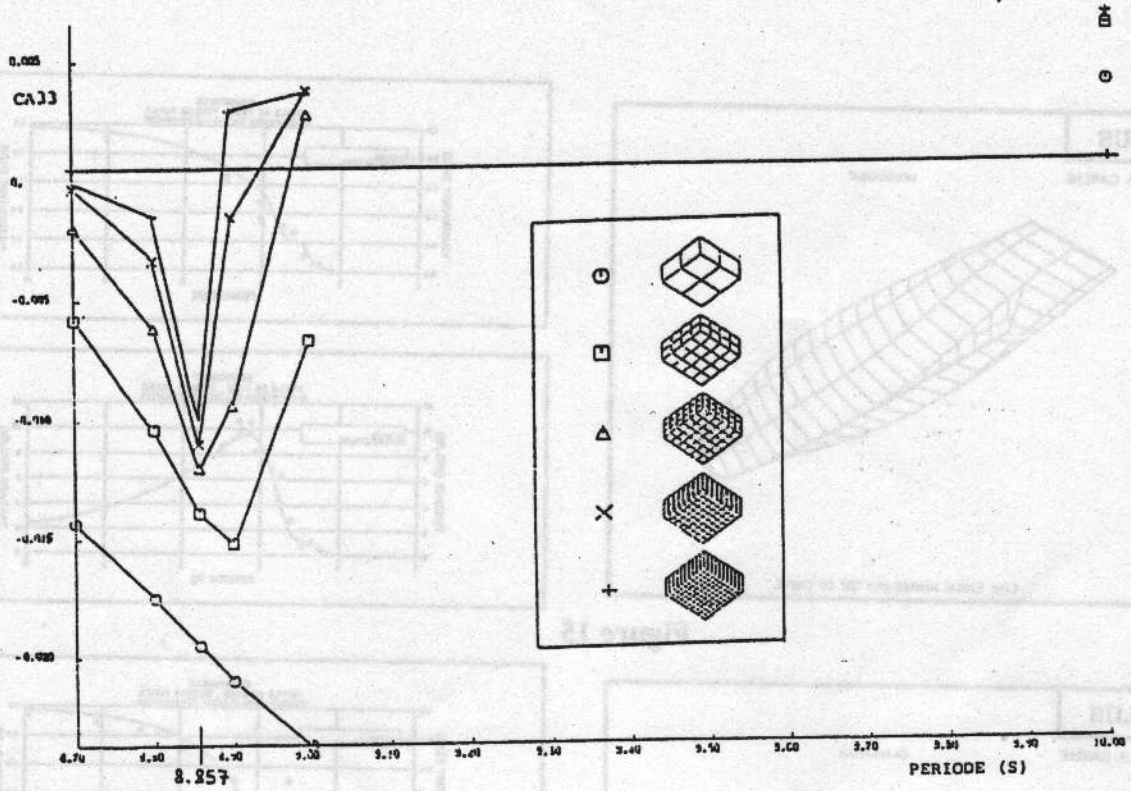


Figure 13

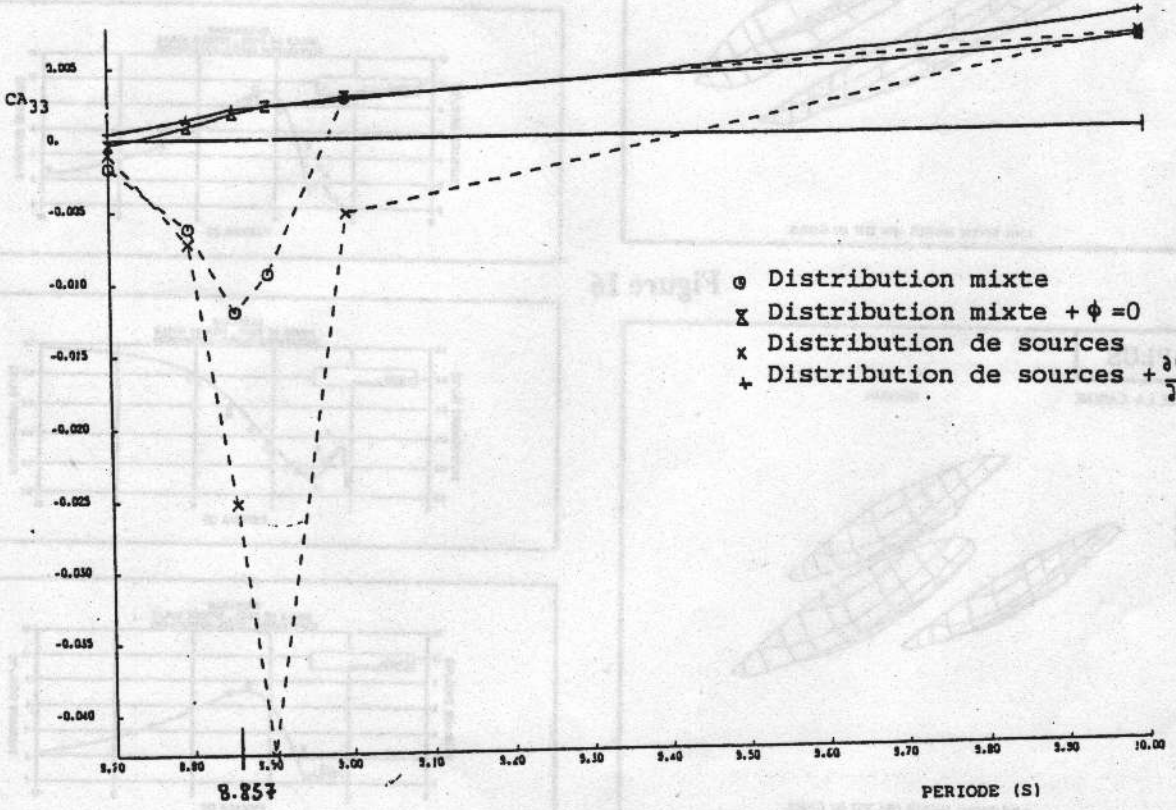


Figure 14

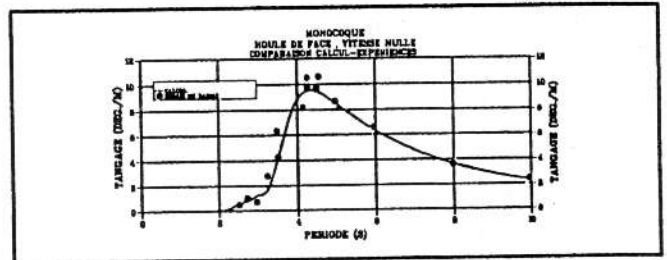
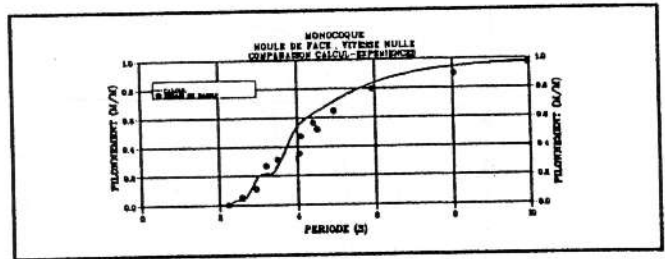
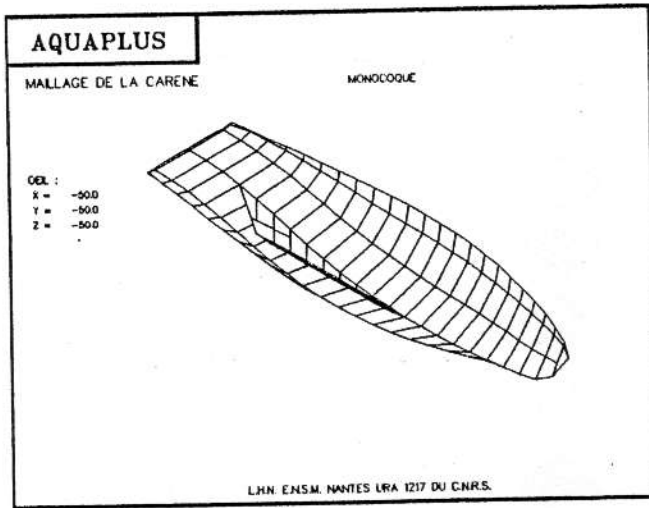


Figure 15

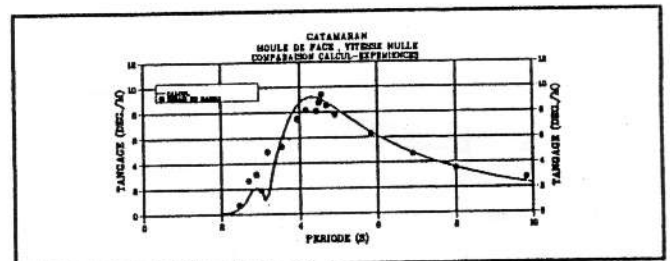
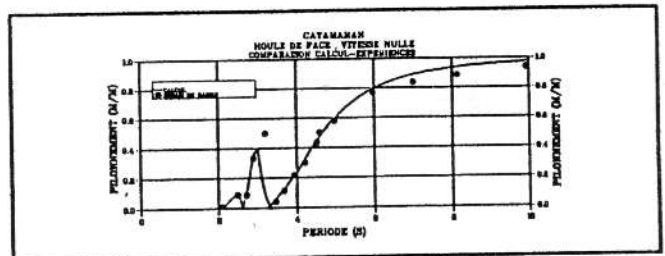
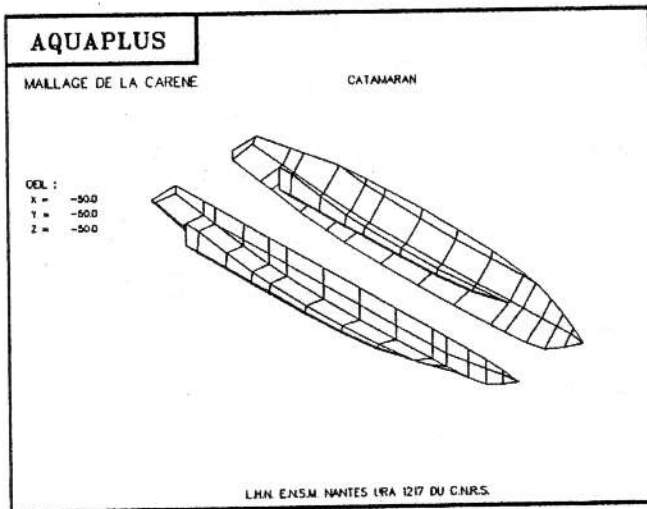


Figure 16

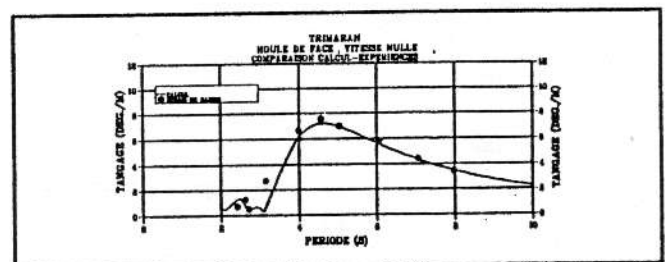
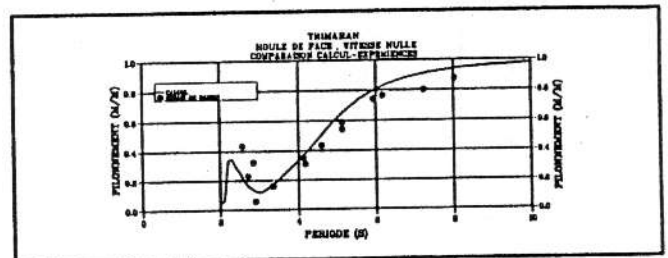
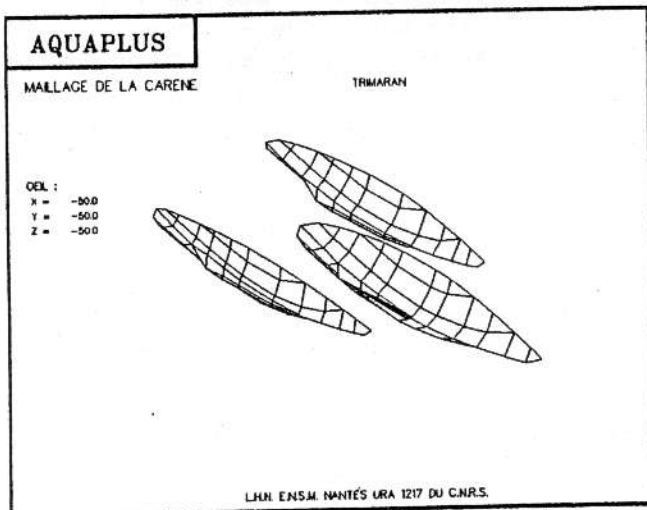


Figure 17

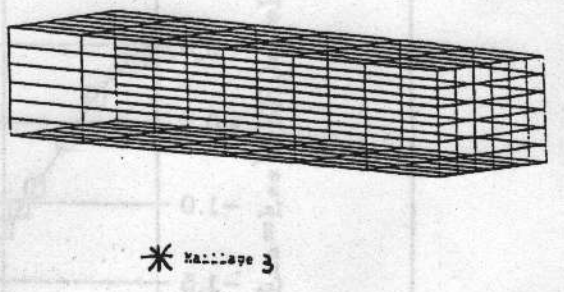
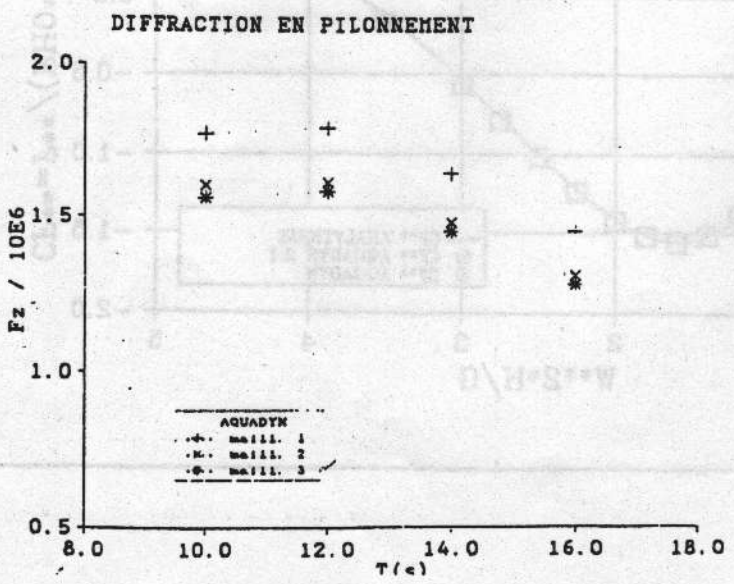
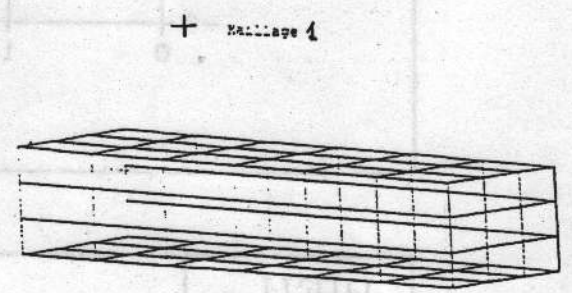
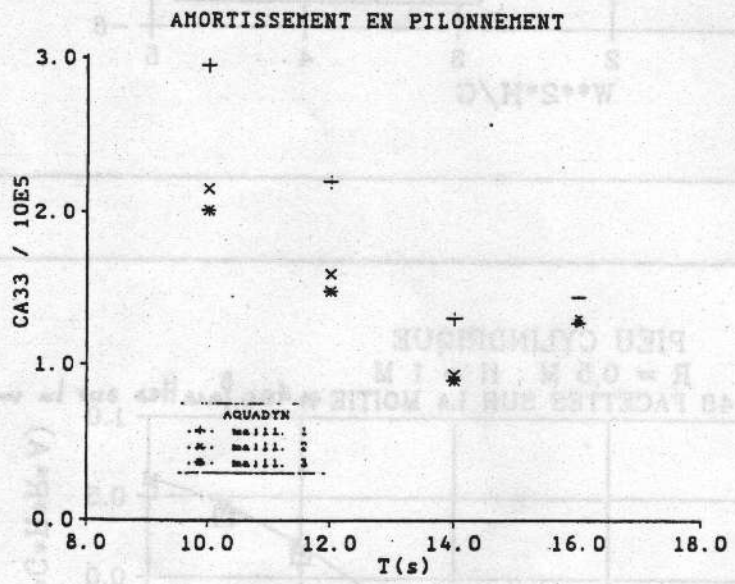
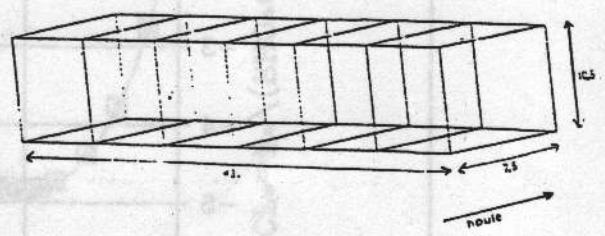
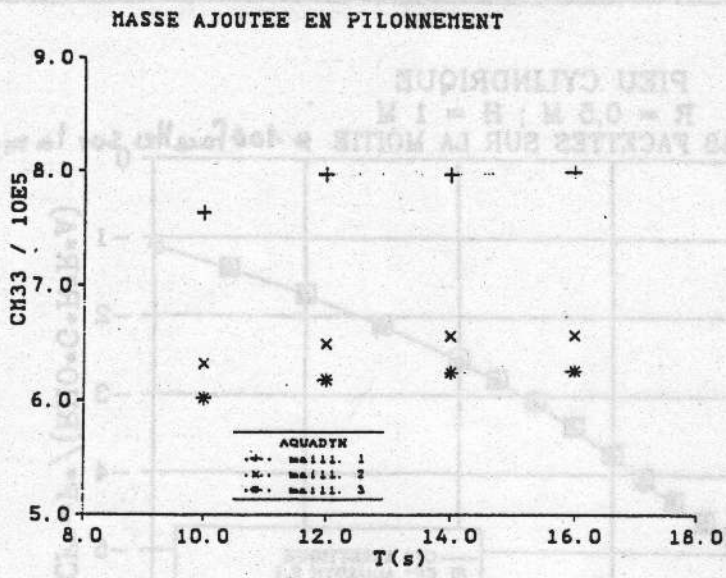


Figure 18

Figure 19

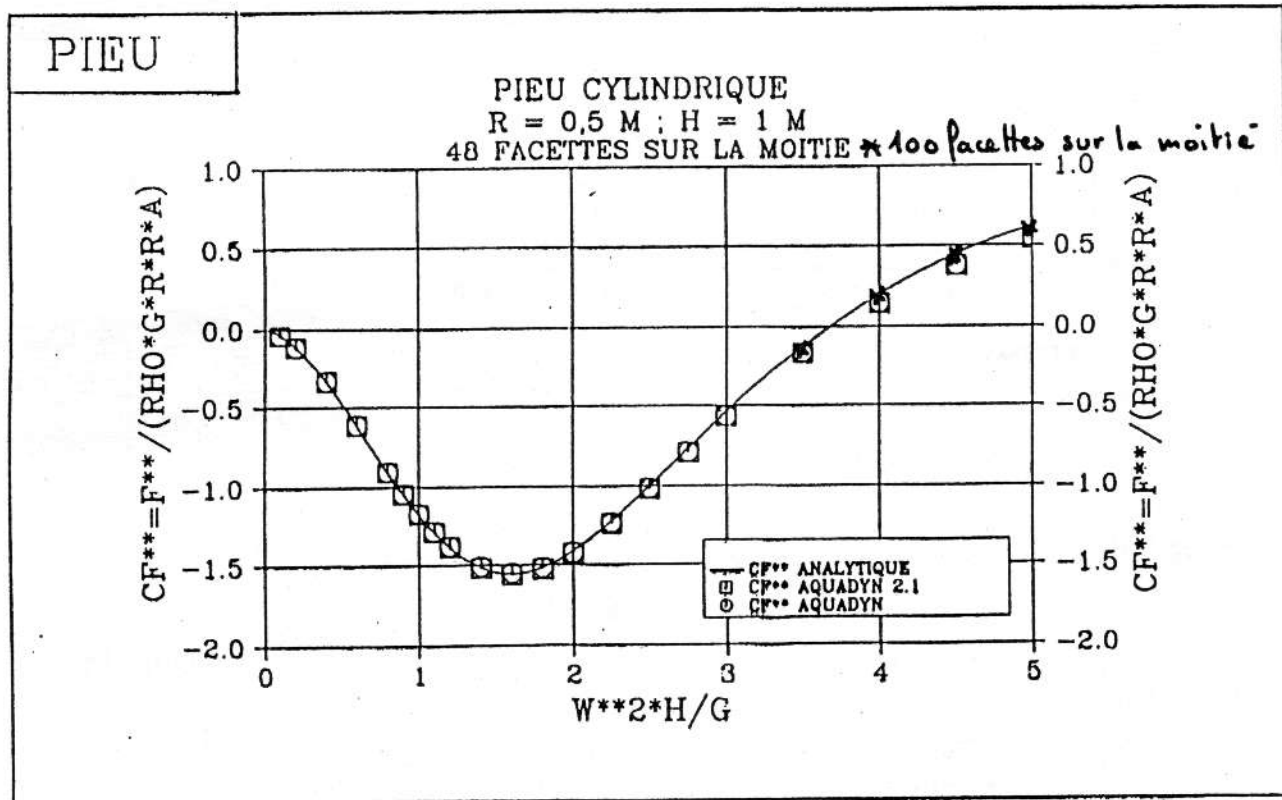
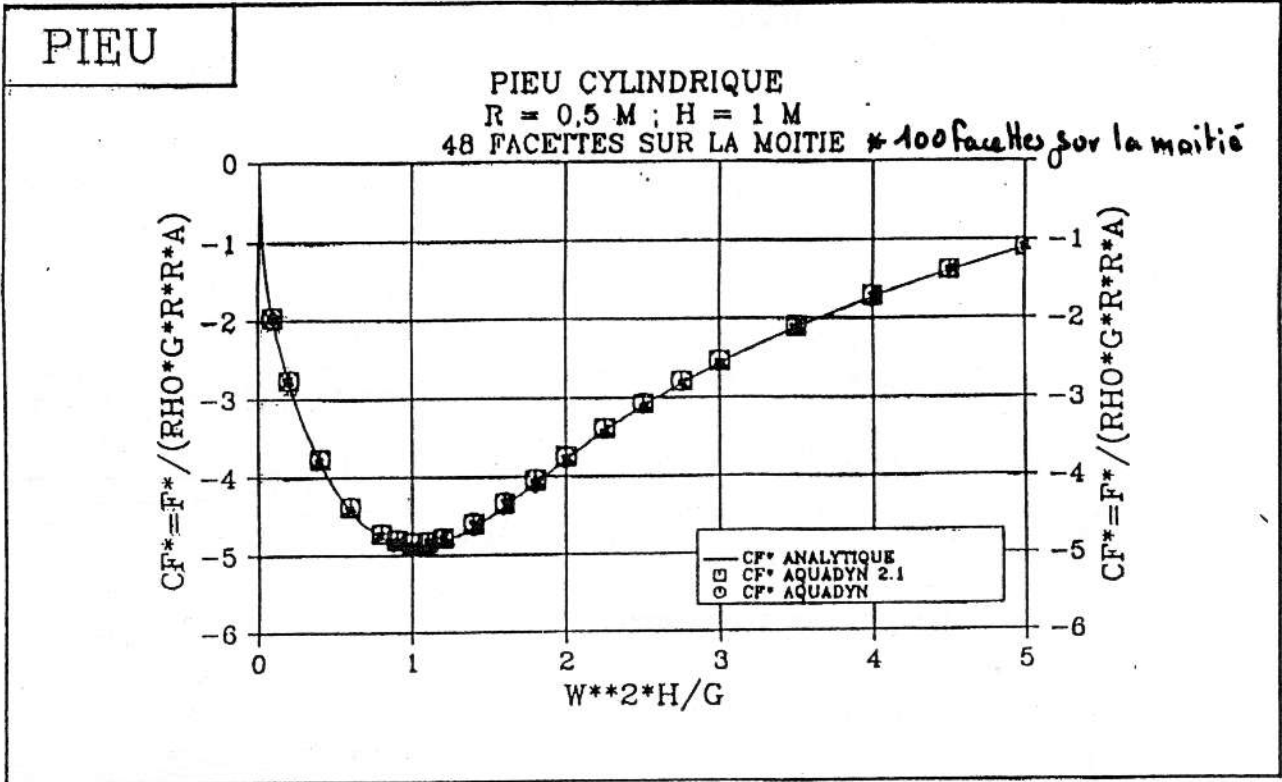
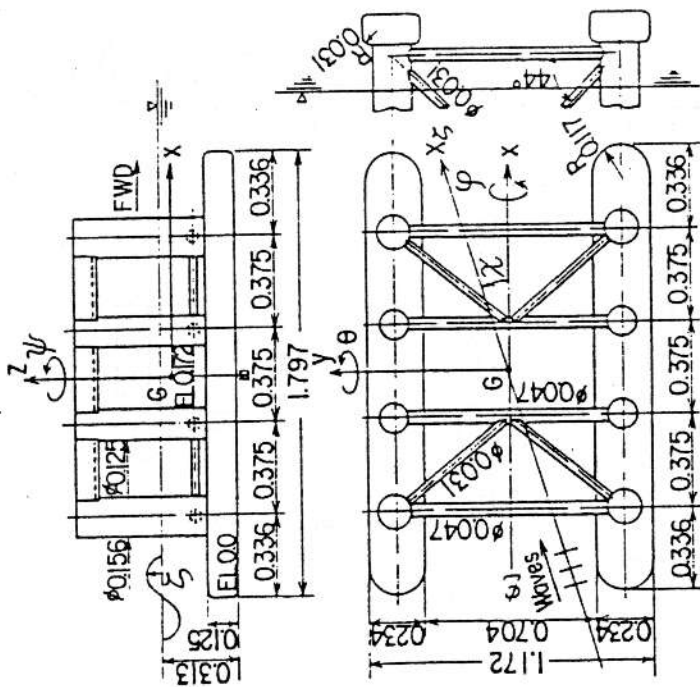


Figure 20

i T T C [2 7]



Wave Elevation $\zeta = \zeta_A \cos(\omega t - kX_s)$
 Motion of Rig $X = X_A \cos(\omega t - \epsilon x)$

Fig. 1 Semi-submersible and coordinate system used in calculation.

AQUADYN: D, E1

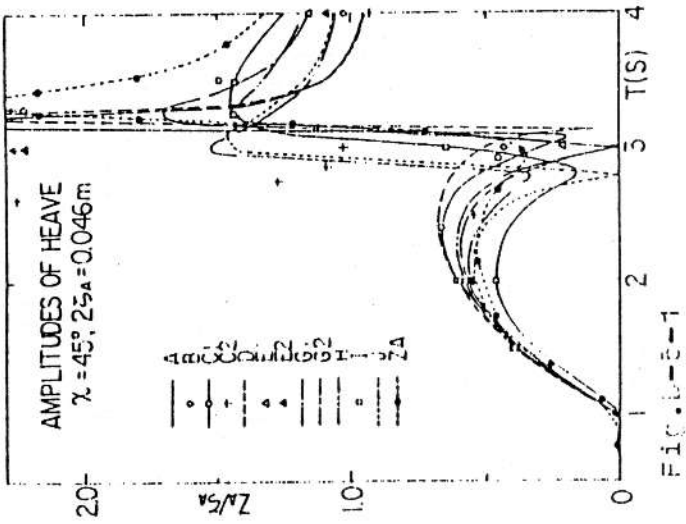


FIG. E-5-1

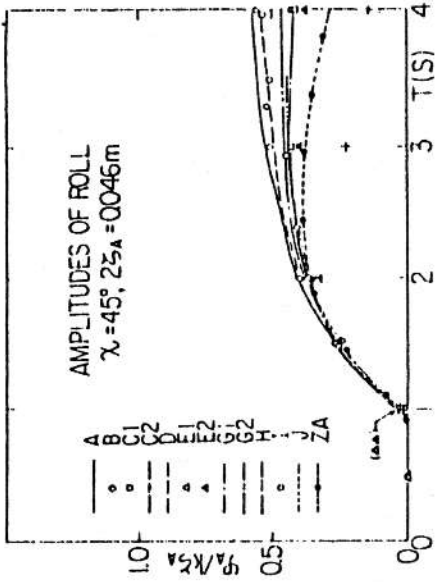


FIG. E-6-1

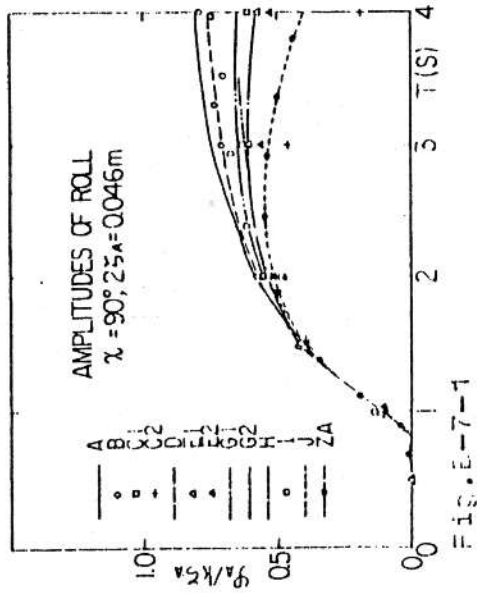


FIG. E-7-1

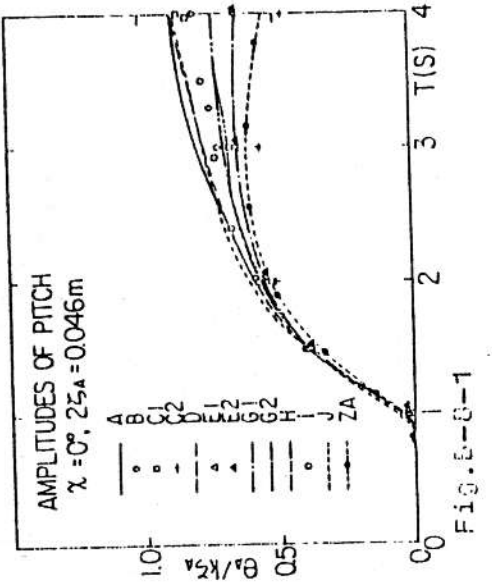


FIG. E-8-1

Figure 21

ISSC [28]

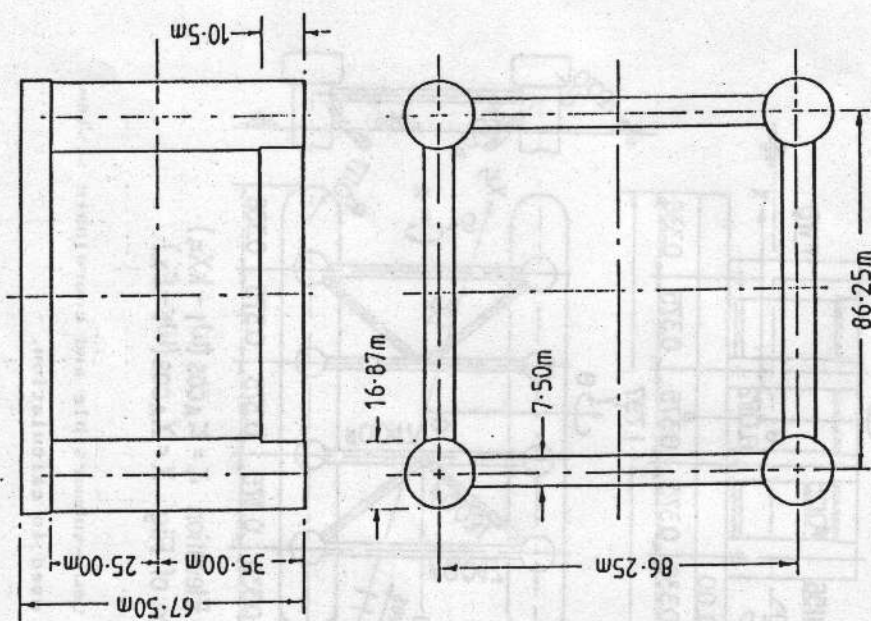


Figure 1. Configuration of TLP case study

AQUADYN: I

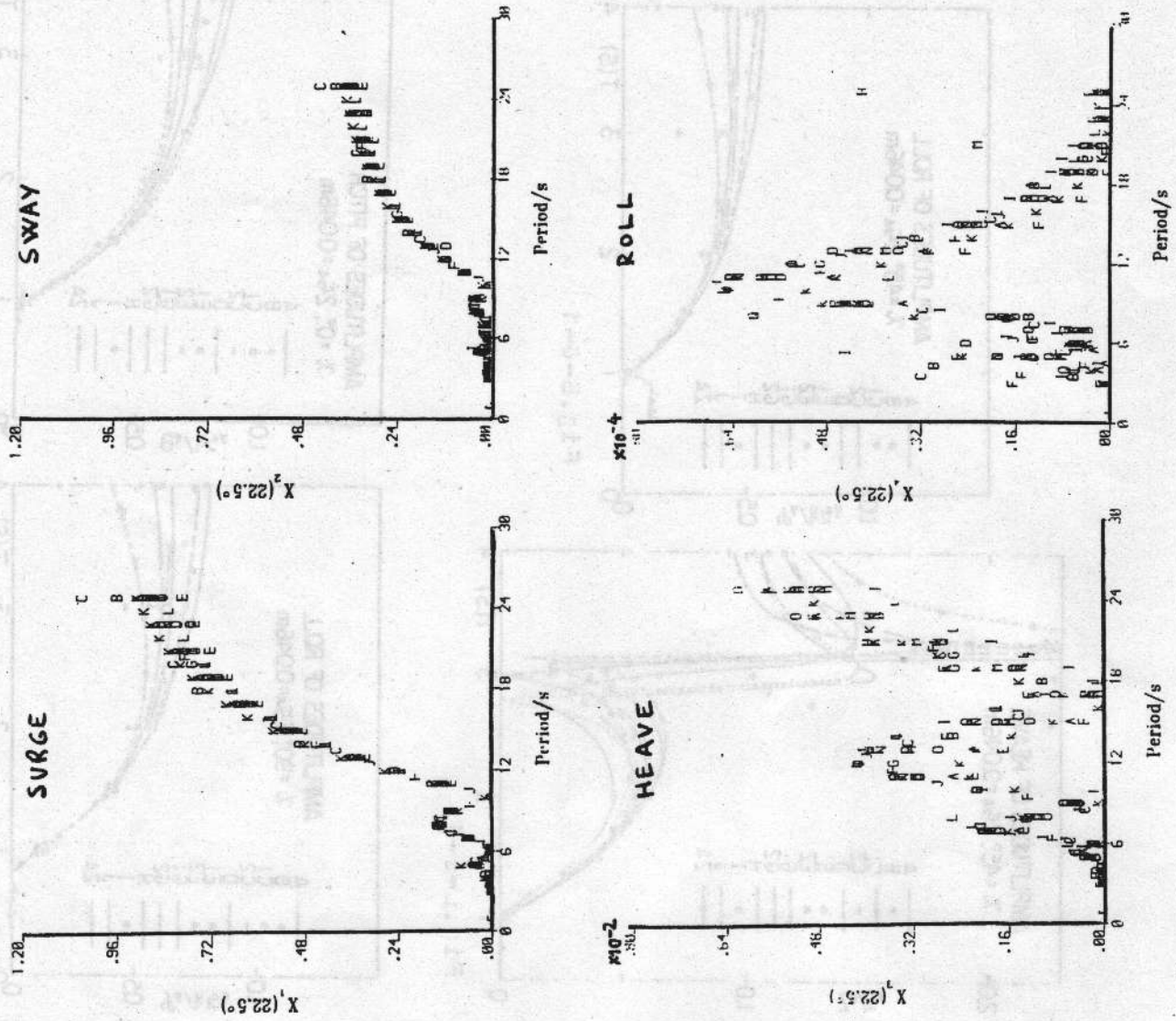
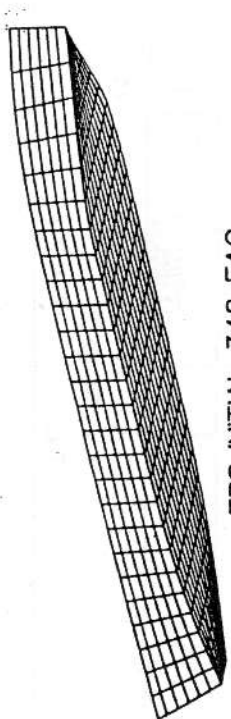
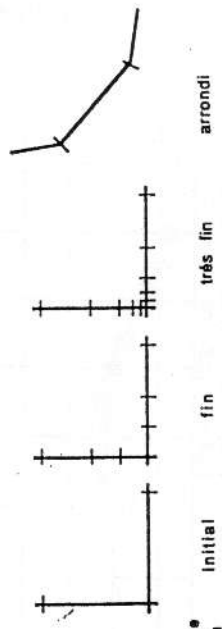


Figure 22



TPS INITIAL 348 FAC.



maillage du coin	Initial	fin	très fin	arrondi
nombre de facettes sur le 1/2 corps	348	512	664	296

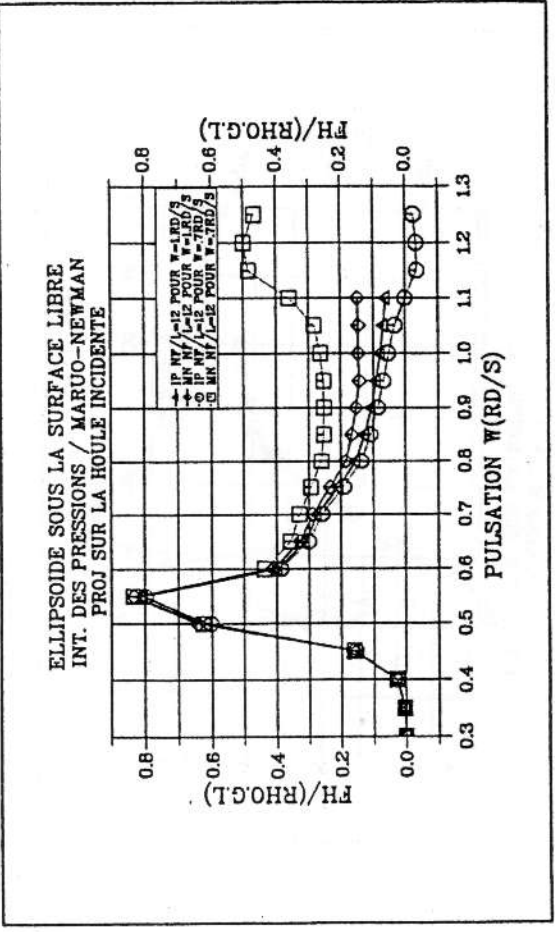
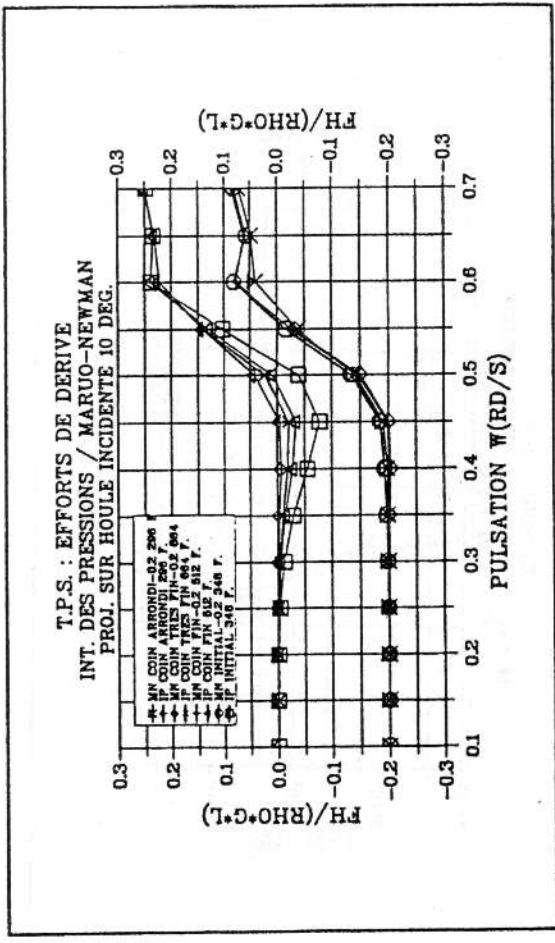
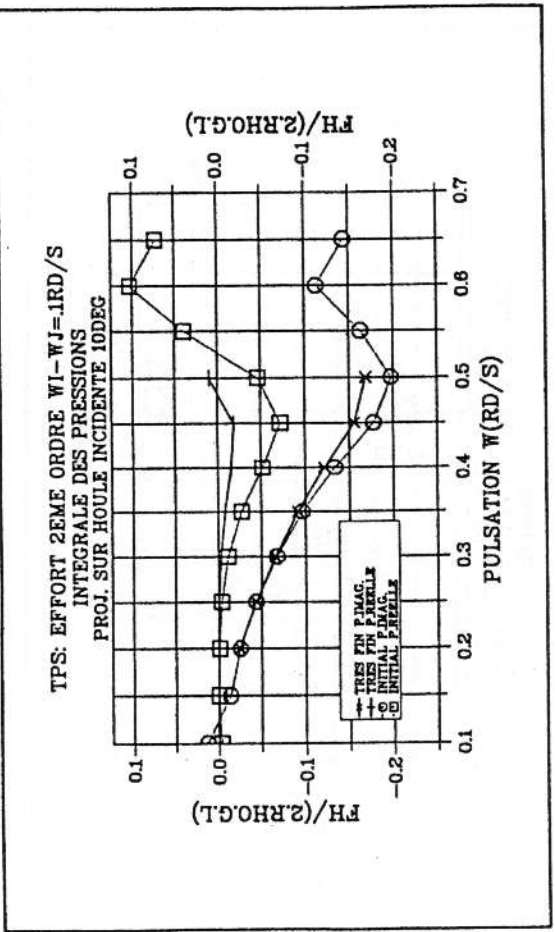


Figure 23

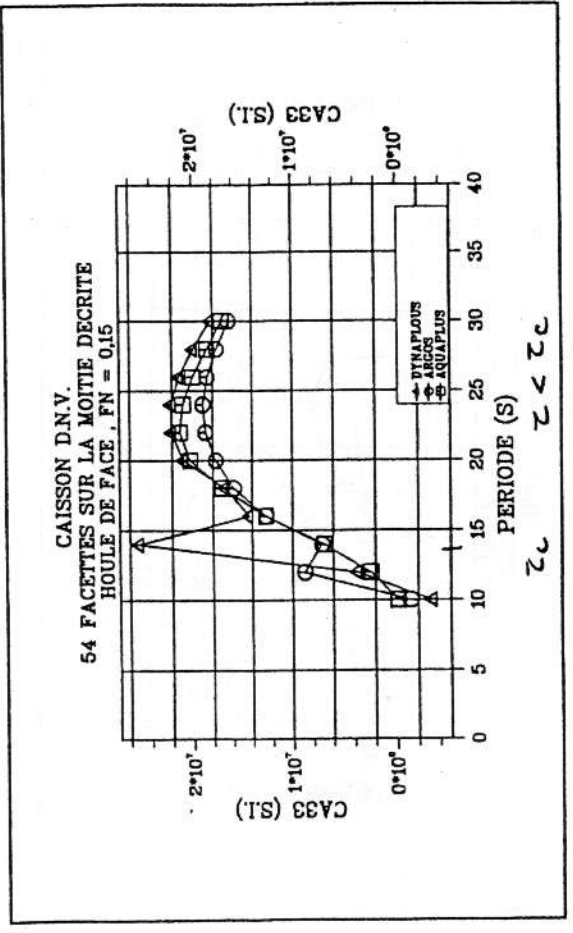
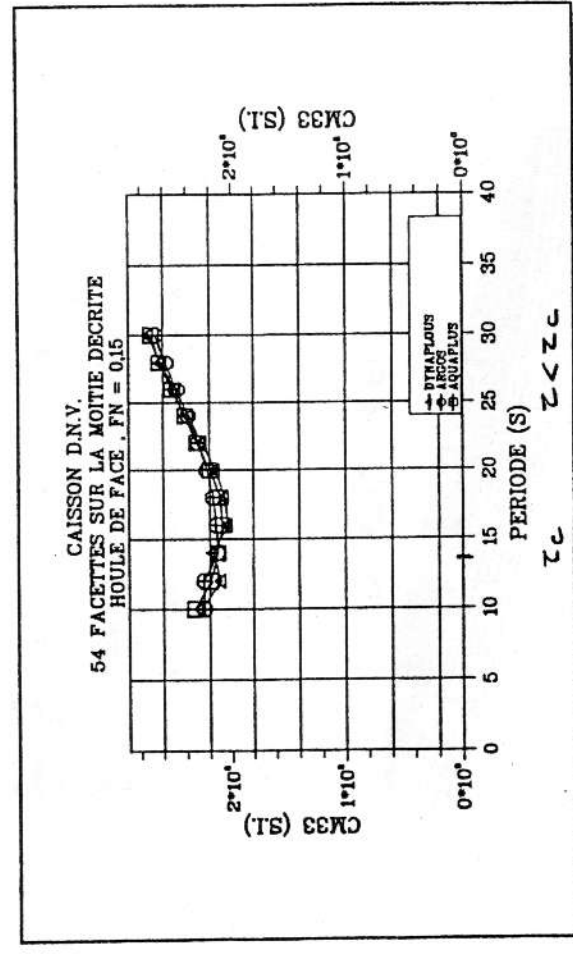
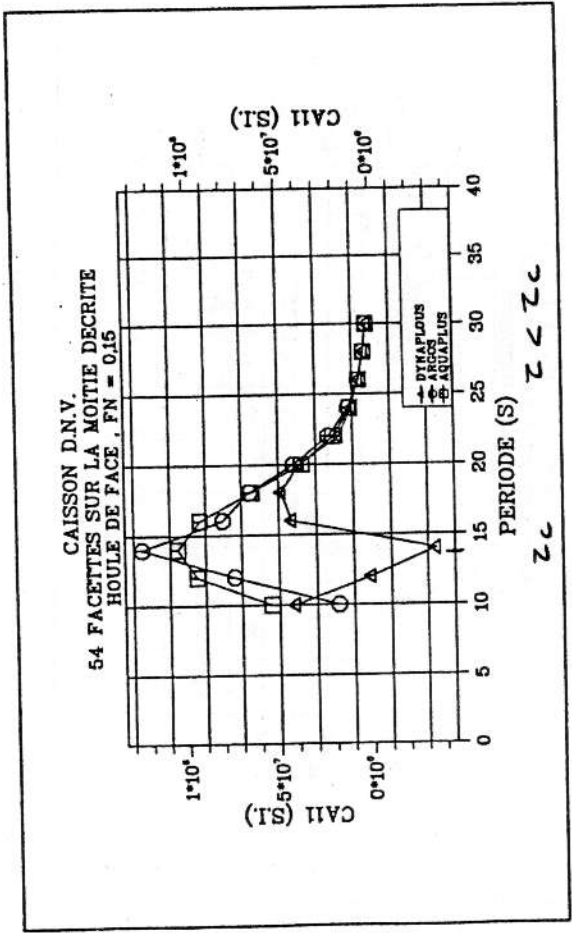
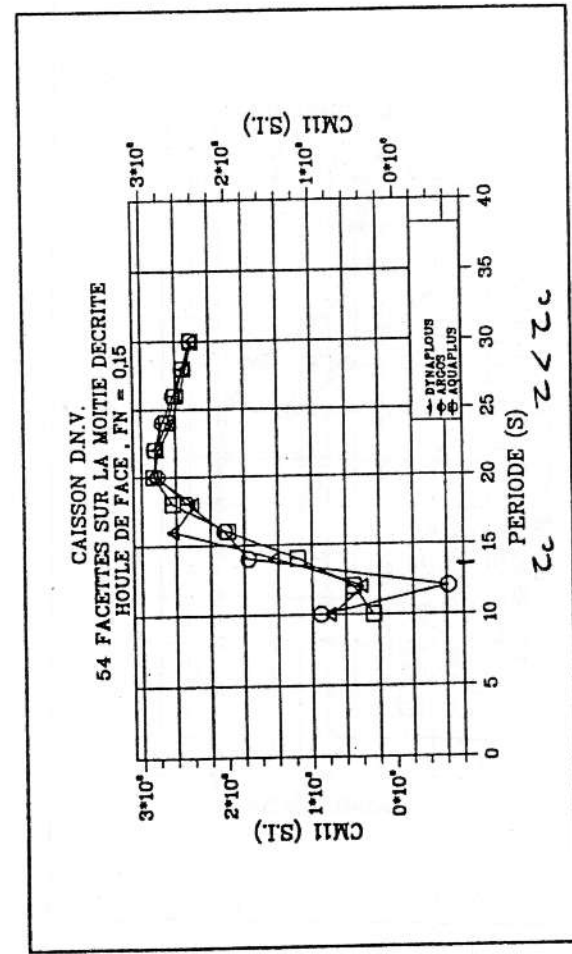


Figure 24

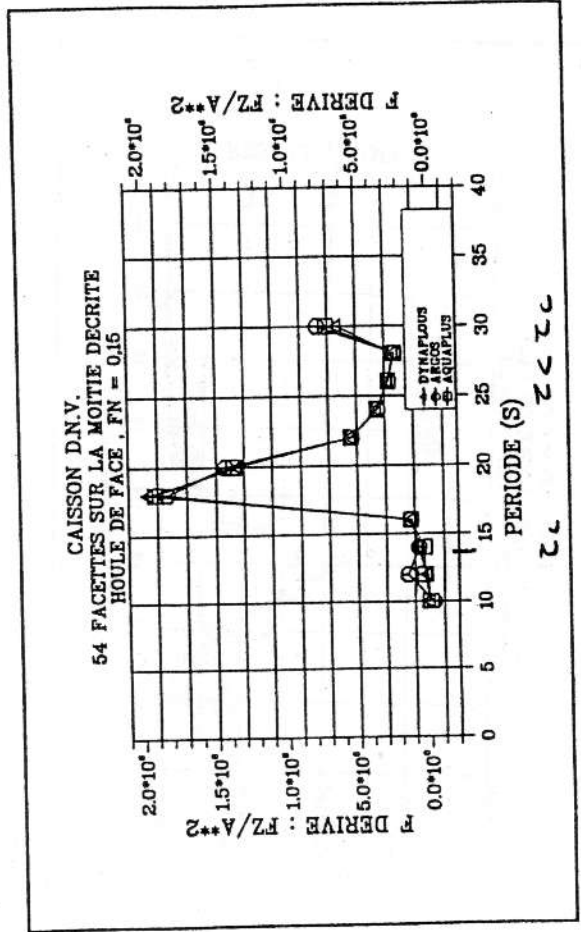
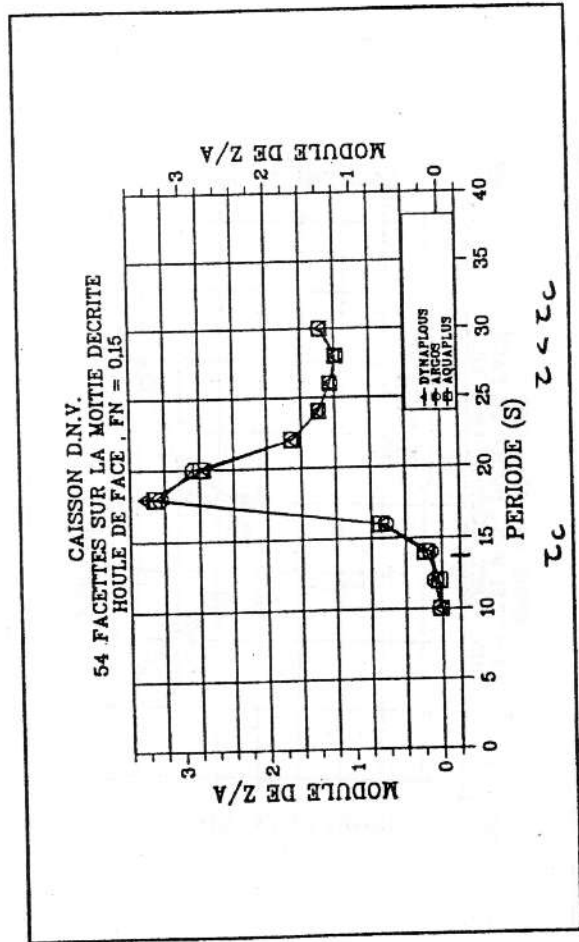
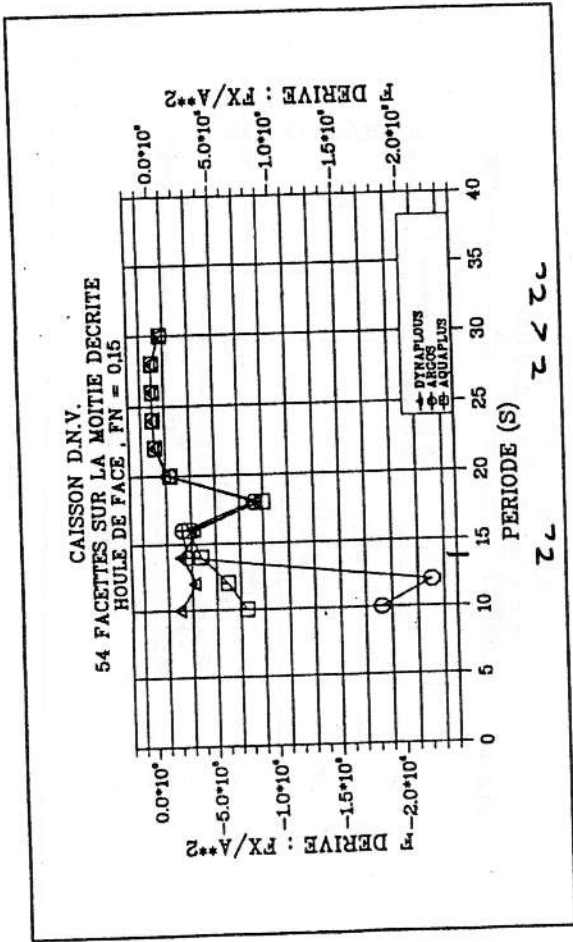
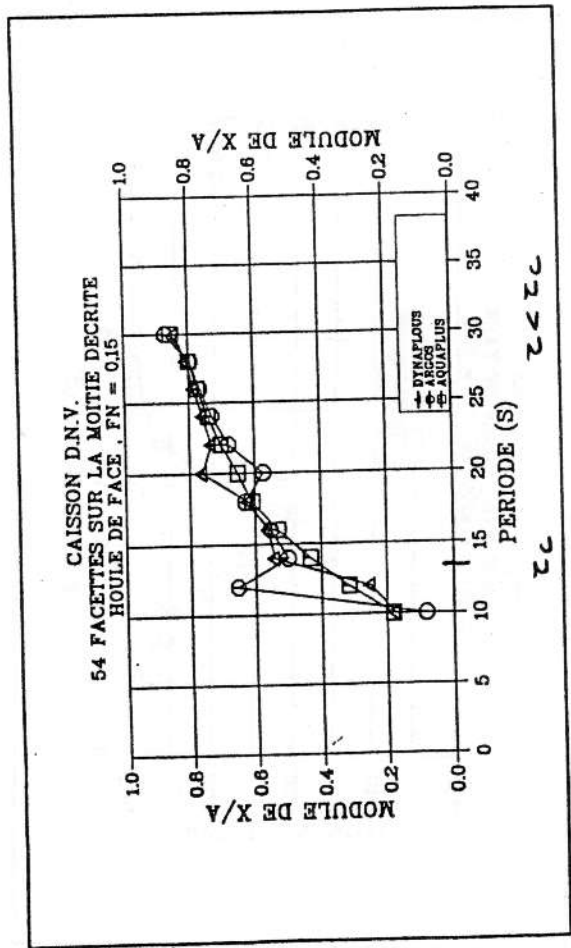


Figure 25

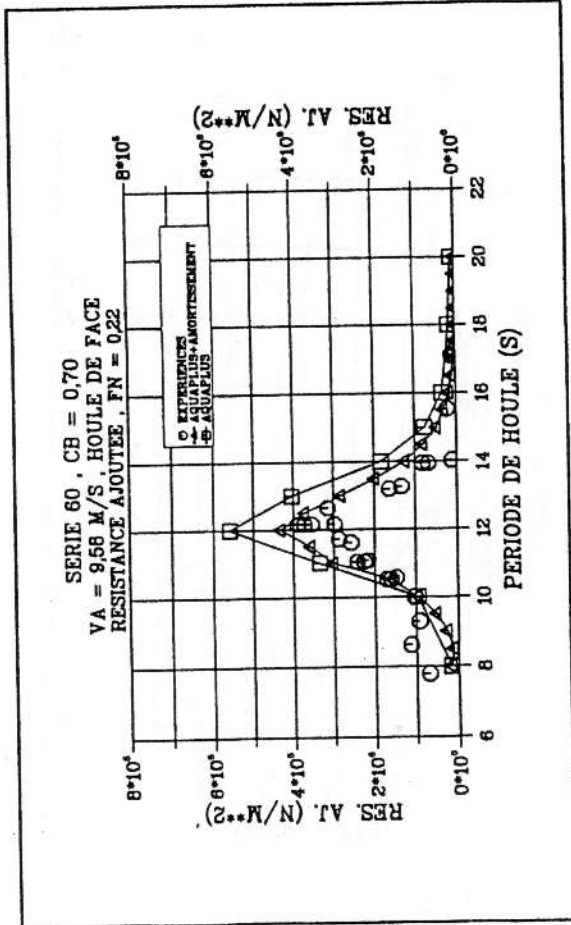
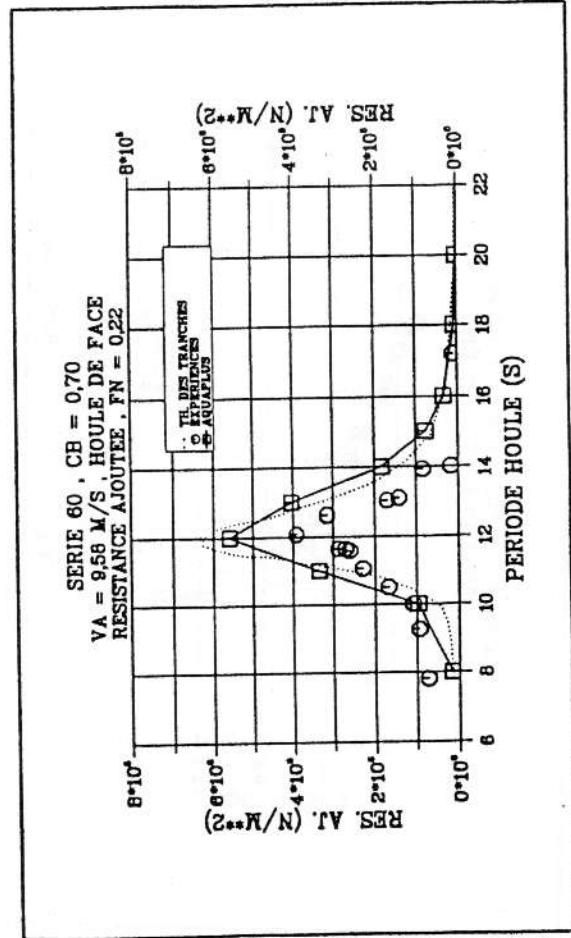
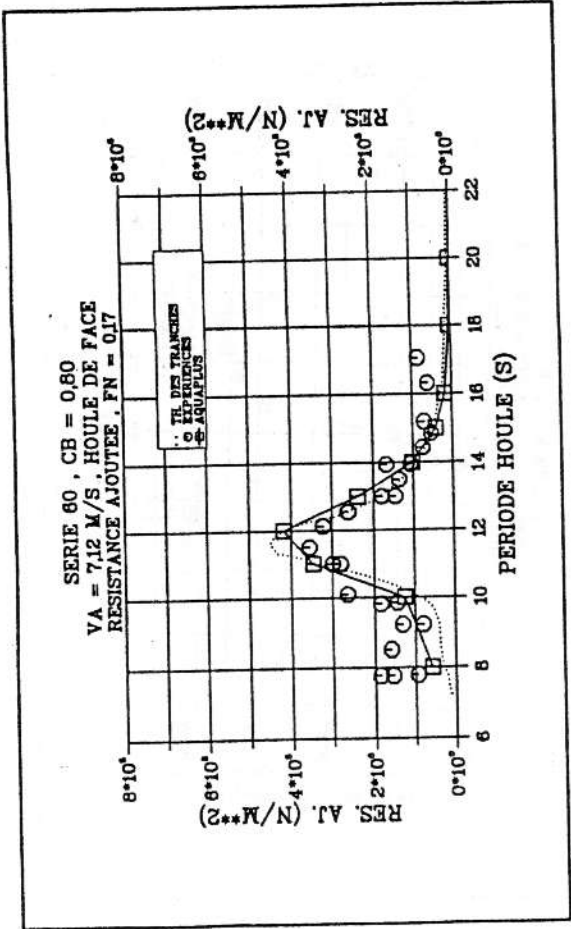
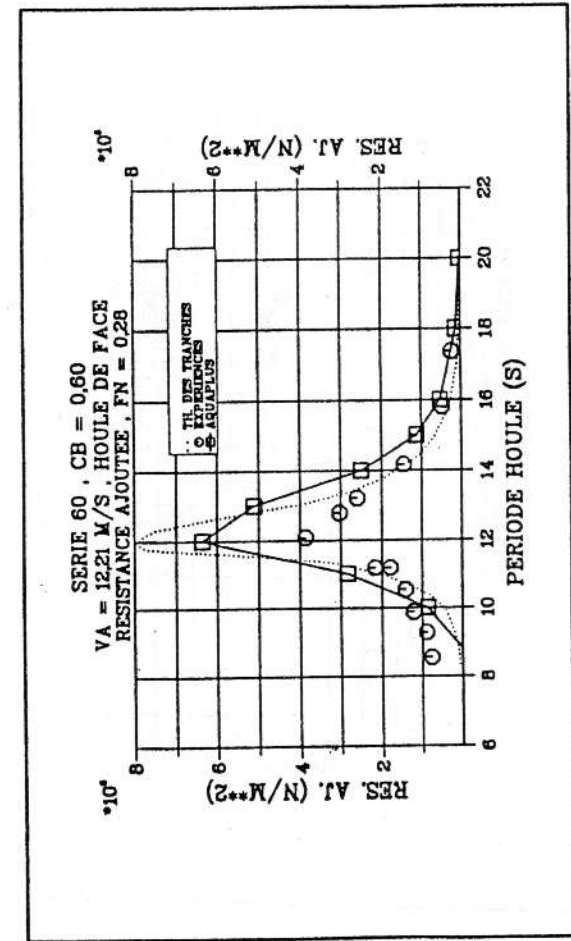
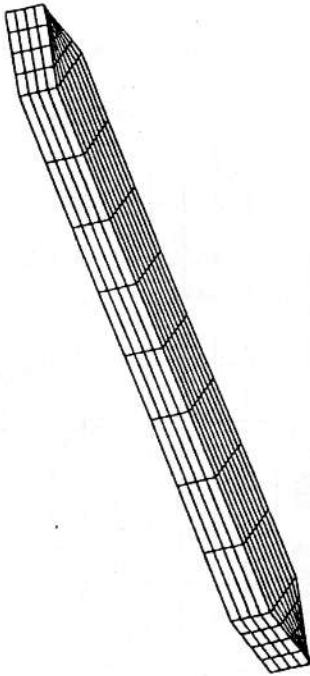


Figure 26



CYLINDRE RECTANGULAIRE

Longueur L = 2,5 m, Largeur B = 0,25 m, Tirant d'eau T = 0,15 m

L' = 2,333 m, T' = 0,25 m, V = 0,08438 m³

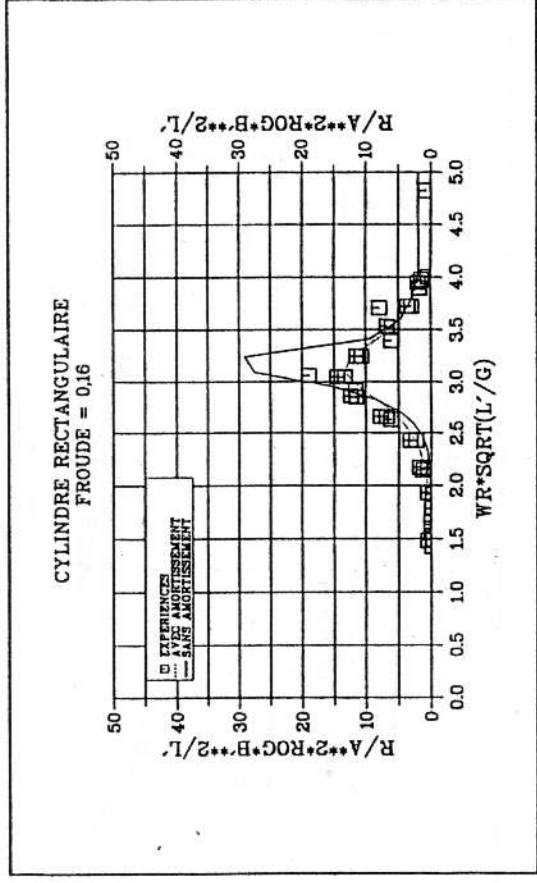
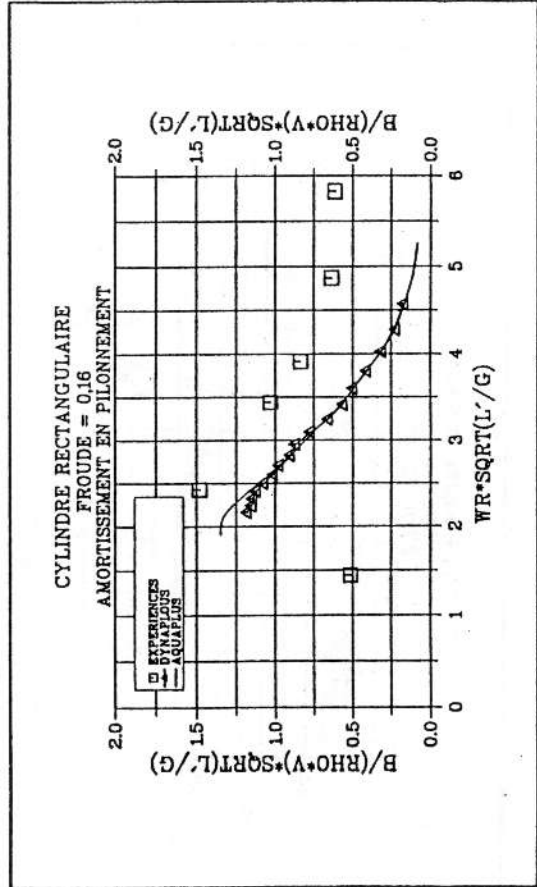
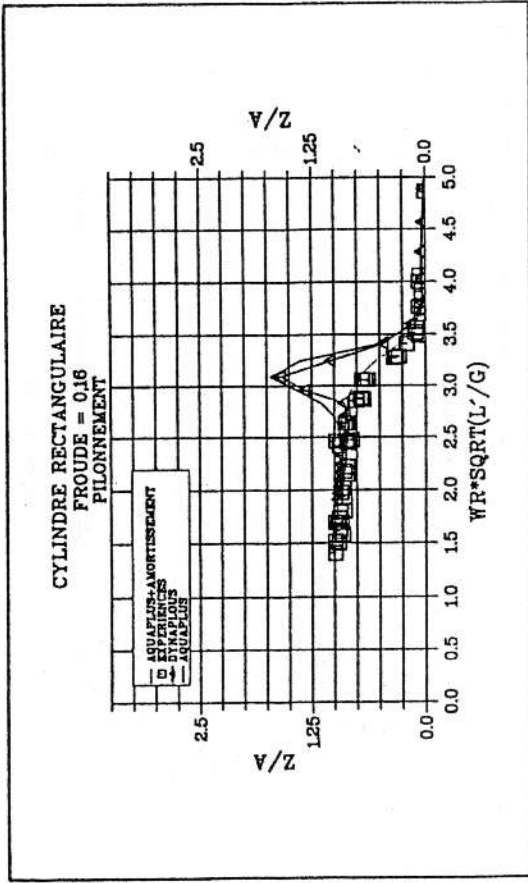


Figure 27

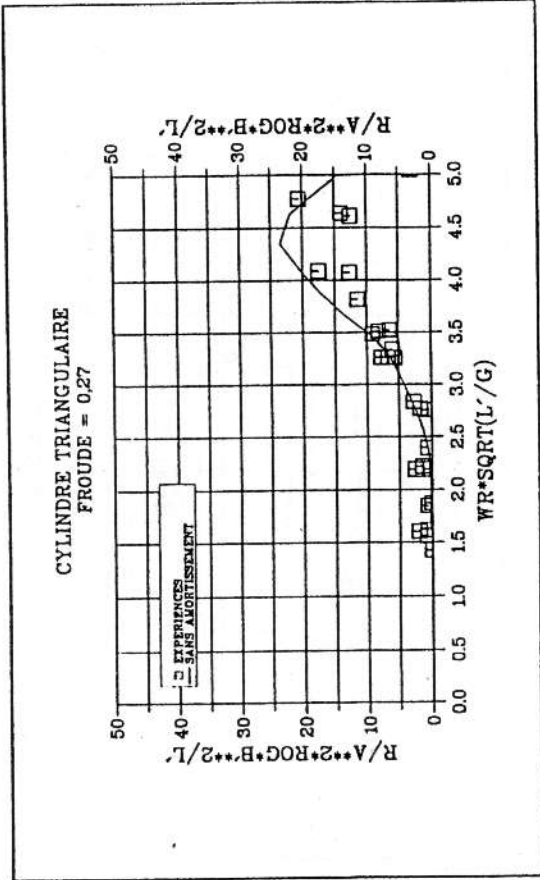
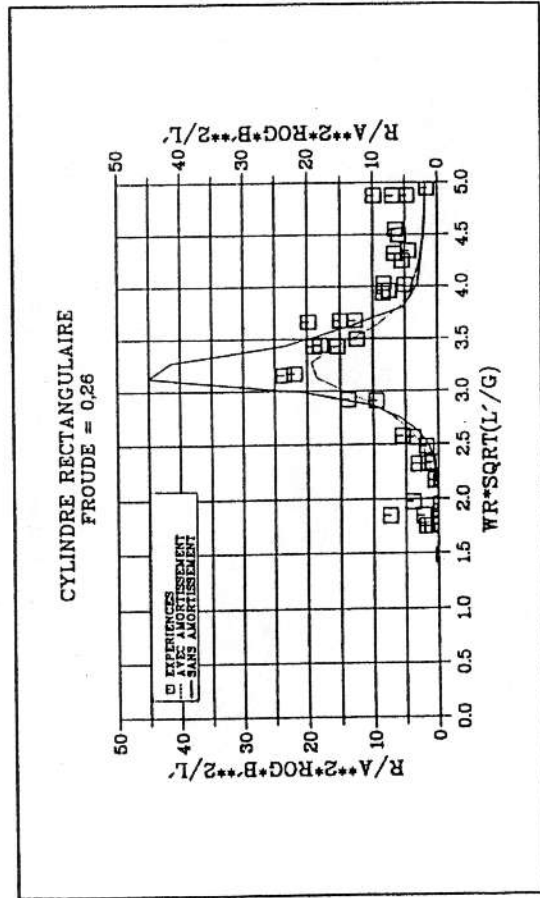
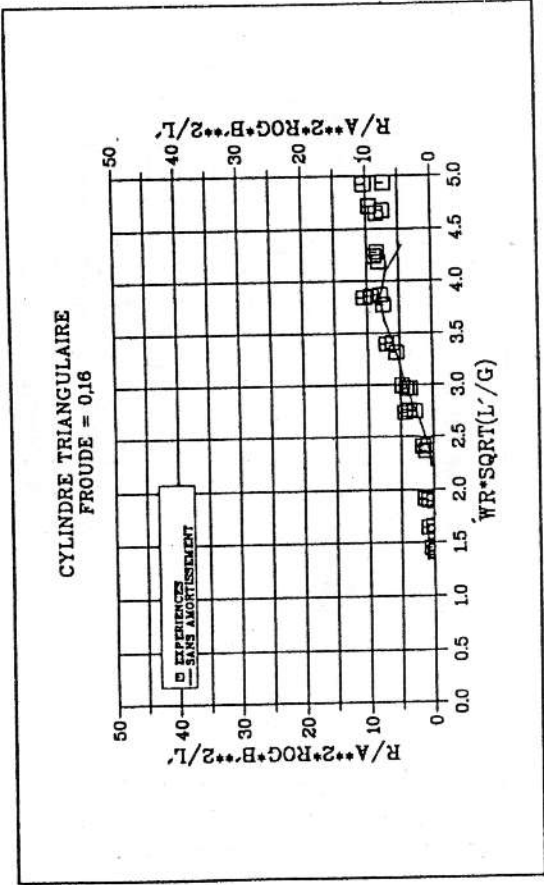
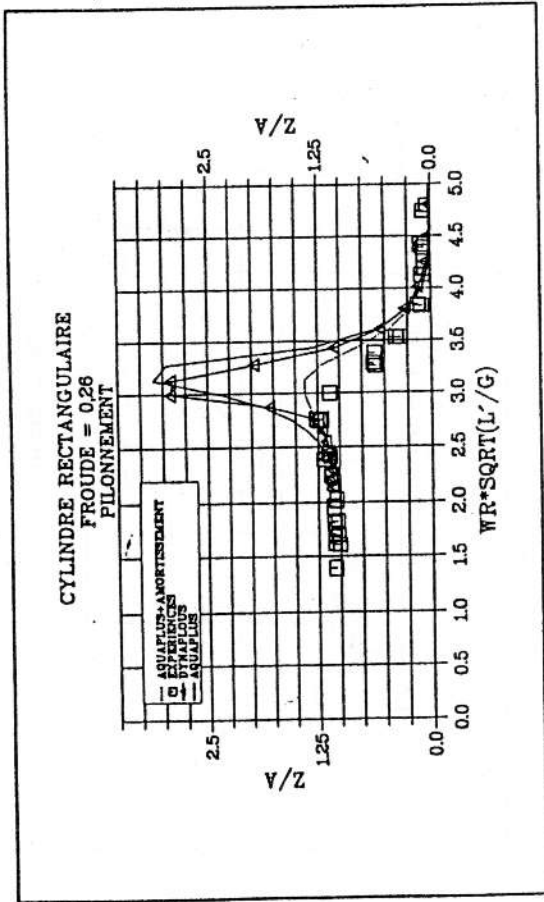


Figure 28

V - CONCLUSIONS:

5.1 Recommended mesh :

The behaviour of all codes is similar. For all the computations at first order, the mesh refinement must be greater than 6 panels per wave length in all directions (x,y,z). This is not always sufficient, especially for bodies with sharp corners. It is necessary to keep in mind that before solving the diffraction-radiation problem we have to solve the potential problem in infinite fluid. If we have no convergence on the solution of this problem, we cannot hope to have an acceptable solution with the body in waves. To obtain a reasonable accuracy in infinite fluid, we must have at least 4 panels on each side of a body (particularly in the thickness of a plate) and a refinement at each local variation of the shape. For simple bodies with a length of the same order as the wave length, a number of panels between 100 and 200 on the described part is generally sufficient.

For the second order problem, drift forces, added resistance or slow drift forces, we must have a more refined mesh. In this case 12 panels per wave length are the minimum. The Maruo-Newman formulation is less sensitive to the number of panels than pressure integration, but we must always try to obtain the agreement between the two formulations to be sure of the quality of the solution.

5.2 Computation time and memory :

All calculations are made in simple precision. The time will be given for a computer VAX 8700 of 6 Mips. The computer VAX 9420 or workstations UNIX type HP 9000-720 or Silicon Graphics are 7 times faster approximately. The computation time can be divided into two parts : one part, the influence coefficients, varying like N^2 and the other part, the resolution of complex linear system, varying like N^3 . It must be noted that to obtain a reliable computing time for all shapes, all the linear systems, real or complex, are solved by the direct Gauss method.

For a mesh of 100 panels one the described part of the body (200 panels on the whole body), the calculation time on VAX 8700 are for one period:

- AQUADYN 2.1 :

Infinite depth :

- 8 s for the terms in $1/R$ (only for the first calculation, this term is stored on disk).
- 6 s for the terms depending of the period.
- 4 s for the radiation problem (2 complex systems 100×103)
- 4 s for the diffraction problem (1 complex system 100×101)
- 6 s for motions and drift forces (calculations+1 complex system 100×101)

Finite depth :

- 4 s for the terms in $1/R$ (only for the first calculation, this term is stored on disk).
- 36 s for the terms depending of the period.
- 4 s for the radiation problem (2 complex systems 100×103)
- 4 s for the diffraction problem (1 complex system 100×101)
- 6 s for motions and drift forces (calculations+1 complex system 100×101)

- AQUAPLUS:

Infinite depth :

- 7 s for the terms in $1/R$ (only for the first calculation, this term is stored on disk).
- 5 s for the terms depending of the period.
- 4 s for the radiation and diffraction problem (2 complex systems 100×104)
- 2 s for motions and drift forces (calculations)

Finite depth :

- 4 s for the terms in $1/R$ (only for the first calculation, this term is stored on disk).
- 20 s for the terms depending of the period.
- 4 s for the radiation and diffraction problem (2 complex systems 100×104)
- 2 s for motions and drift forces (calculations)

To obtain a transfer function with good accuracy, 10 to 20 periods are needed.

For more than 200 panels, the main computing time is in the resolution of linear systems. It can be seen that AQUAPLUS is asymptotically 1.5 times faster than AQUADYN 2.1. If there are several wave incidence at zero forward speed, the ratio can be greater, because calculations for all incidence are made in the same linear system in AQUAPLUS instead of solving as many systems as the number of incidences in AQUADYN 2.1. For memory, the old version AQUADYN was 50 slower than AQUADYN 2.1 for influence coefficient calculations. The current seakeeping code is now AQUAPLUS and all the developments are made on this code. The CUVE code solves only real linear systems of the same size as in AQUAPLUS (a little greater as the free surface has to be meshed), the computing time are then approximately 2 times faster than the time for solving the radiation problem in AQUADYN 2.1.

The standard parameters of the current version of AQUAPLUS are 1000 panels on the described part, located on a maximum of 8 bodies with independent motions with a maximum of 24 wave incidence. For these parameters, the size of central memory needed for computation is less than 15 MBytes (this is the size used by PREK) with 150 MBytes of storage of temporary and permanent files on disk for a series of calculations. All these sizes are proportional to N^2 . To day, the greatest case computed was 2300 panels on the half of the body. For one period, it takes approximately 45 minutes on VAX 9420.

5.3 Conclusions and perspectives:

To day, the behaviour of linear seakeeping codes is well known for zero forward speed. These codes are able to predict the first order quantities with an accuracy of the order of 10 %, which is generally sufficient. They give the amplitude of motions outside the resonance frequencies and location of the resonance frequencies. The first improvement of these codes would be to find a method of resolution of complex linear systems with several second members fast and reliable. To-day, all the methods tried, like bi-conjugate gradient with or without preconditioning, are not satisfactory. If they are sometimes faster, it is not the case with all shapes. Moreover, these methods are iterative methods, which seems not suitable for a great number of second members. The other improvement is to take into account in these codes the viscous damping at resonance to get an estimation of the response. This can be done by experimental means in wave tanks or by computation codes solving Navier-Stokes equations. For the calculation of second order forces, there is still some problem for bodies with sharp angles near the free surface. In this case, the agreement between Maruo-Newman formulation and pressure integration is not always good. The Maruo-Newman formulation gives better results since the forces have their theoretical sign, but all quantities are not known when using these formulas. Research has to be made to insure the validity of calculations by pressure integration. With forward speed, the problem is not entirely solved to day. The approximation of the linear free surface condition used in AQUAPLUS gives good values of added resistance when the motions are exact. The knowledge of viscous damping is again needed. The exact linear free surface condition is very difficult to use at realistic speeds, due to strongly oscillating character of the integration term in calculation of influence coefficients. Perhaps the Rankine source method would be an interesting alternative to the Kelvin source method in this case, if the problem resulting from the numerical absorption of the radiated waves is correctly solved. Research on the problem with forward speed must be carried on.

BIBLIOGRAPHY :

- [1] T.H. HAVELOCK , 1942, "The drifting force on a ship among waves" - Phil. Mag., Vol. 33, 1942
- [2] B.V. KORVIN-KROUKOWSKI and W.R. JACOBS, 1957, "Pitching and heaving motions of a ship in waves" - Trans. SNAME, Vol. 65, 1957
- [3] N. SALVESEN, E.O. TUCK, O. FALTINSEN, 1970, "Ship motions and sea loads" - Trans. SNAME, Vol. 78, 1970

- [4] J.STROM-TEJSEN, H.Y.H. YEH, D.D. MORAN, 1973, "Added Resistance in Waves" - Trans. SNAME, Vol. 81, 1973
- [5] M.S. CHANG, 1977, "Computation of three-dimensionnal ship motions with forward speed" - 2nd Int. conf. on Numerical Ship Hydrodynamics, University of Berkeley, 1977
- [6] J.N. NEWMAN, 1978, "The theory of ship motions" - Advances in applied mechanics, Vol. 18, 1978
- [7] J. BOUGIS, 1980, "Etude de la diffraction-radiation dans le cas d'un flotteur indéformable animé d'une vitesse moyenne constante et sollicité par une houle sinusoïdale de faible amplitude" - Thèse de Docteur-Ingénieur, E.N.S.M. Nantes, 1980
- [8] A. GREKAS, 1981, "Contribution à l'étude théorique et expérimentale des efforts du second ordre et du comportement dynamique d'une structure marine sollicitée par une houle régulière et un courant" - Thèse de Docteur-Ingénieur, E.N.S.M. Nantes, 1981
- [9] P. GUEVEL, A. GREKAS, 1981, "Le théorème de Lagally généralisé et ses applications en hydrodynamique navale" - Bulletin de l'A.T.M.A. n° 81, A.T.M.A., Paris, 1981
- [10] P. GUEVEL, J. BOUGIS, 1982, "Ship motions with forward speed in infinite depth" - Int. Shipbuilding Progress, Vol. 29, 1982
- [11] W. BEUKELMAN, 1983, "Vertical motions and added resistance of a rectangular and triangular cylinder in waves" - Report n° 594, Technische Hogeschool Delft, 1983
- [12] R.H.M. HUIJSMANS, A.J. HERMANS, 1985, "A fast algorithm for computation of 3-D ship motions at moderate forward speed" - 4th Int. Conf. on Numerical Ship Hydrodynamics, Washington, 1985
- [13] G. DELHOMMEQU., J.M. KOBUS, 1987, "Méthode approchée de calcul du comportement sur houle avec vitesse d'avance" - Bulletin de l'A.T.M.A. n° 87, A.T.M.A., Paris, 1987
- [14] G. DELHOMMEAU, 1987, "Les problèmes de diffraction-radiation et de résistance de vagues : étude théorique et résolution numérique par la méthode des singularités" - Thèse de Docteur ès Sciences, E.N.S.M. Nantes, 1987
- [15] R. ZHAO, O. FALTINSEN, 1989, "Interaction between current, waves and marine structures" - 5th Int. Conf. on Numerical Ship Hydrodynamics, Hiroshima, 1989
- [16] R.F. BECK, A.R. MAGEE, 1990, "Time-domain analysis for predicting ship motions" - I.U.T.A.M., Londres, 1990

- [17] J.N. NEWMAN 1990, "The evaluation of free surface Green functions" - Fourth International Conference on Numerical Ship Hydrodynamics, Washington, 1985
- [18] J.V. WEHAUSEN and E.LAITONE, 1960, "Surface waves" Handbuch der Physik, Vol. IX, 1960
- [19] P. GUEVEL , J.C. DAUBISSE, G. DELHOMMEAU., 1978 , "Oscillations des corps flottants soumis aux actions de la houle" - Bulletin de l'A.T.M.A. n° 78, A.T.M.A., Paris, 1978
- [20] G. DELHOMMEAU 1984 , "Calcul des efforts de dérive sur un ensemble de corps" - Bulletin de l'A.T.M.A. n° 84, A.T.M.A., Paris, 1984
- [21] G. DELHOMMEAU, 1989 , "Amélioration des performances des codes de calcul de diffraction-radiation au premier ordre" , Deuxièmes Journées de l'Hydrodynamique , Nantes , 1989
- [22] G. DELHOMMEAU, 1991 , "Comparaison de différentes approximations du problème de diffraction-radiation avec vitesse d'avance" , Troisièmes Journées de l'Hydrodynamique , Grenoble , 1991
- [23] P. GUEVEL et al;, 1986 , "La récupération de l'énergie des vagues" - Mémorial de l'Artillerie française, Sciences et Techniques de l'Armement 60, 1er Fasc, 1986
- [24] G. DELHOMMEAU, P. FERRANT, M. GUILBAUD, 1992 , "Calculation and measurements of forces on a high speed vehicle in forced pitch and heave" , Applied Ocean Research , 14 (1992), pp 119-126
- [25] J.A. PINKSTER , 1983 , "Low frequency second order wave exciting forces on floating structures" , Publication n° 650, NSMB, Wageningen, 1983
- [26] G. SUSBIELLES, C. BERHAULT , 1978 , "Comparaison des modèles numériques tridimensionnels de diffraction-radiation" , Revue de l'Institut Français du Pétrole, XXXIII(1978), pp. 537-555
- [27] TAKAGI and al , "A comparison of methods for calculating the motion of a semi-submersible", Ocean Engng., 12 (1985), pp. 45-97
- [28] EATOCK-TAYLOR R. and JEFFERYS E.R. , "Variability of hydrodynamic load predictions for a tension leg platform", Ocean Engng., 13 (1985), pp. 449-490
- [29] Workshop on comparative study of computer programs, Norsk Hydro Research Centre, Bergen, Norway, 30 November 1989-1 December 1989.